

Discovery and Optimization of Novel SUCNR1 Inhibitors: Design of Zwitterionic Derivatives with a Salt Bridge for the Improvement of Oral Exposure

Juraj Velcicky,* Rainer Wilcken, Simona Cotesta, Philipp Janser, Achim Schlapbach, Trixie Wagner, Philippe Piechon, Frederic Villard, Rochdi Bouhelal, Fabian Piller, Stephanie Harlfinger, Rowan Stringer, Dominique Fehlmann, Klemens Kaupmann, Amanda Littlewood-Evans, Matthias Haffke, and Nina Gommermann



Cite This: <https://dx.doi.org/10.1021/acs.jmedchem.0c01020>



Read Online

ACCESS |



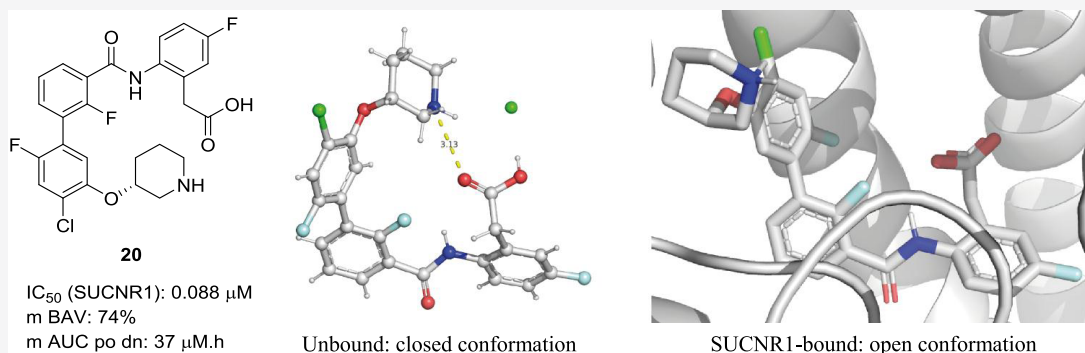
Metrics & More



Article Recommendations



Supporting Information



ABSTRACT: G-protein-coupled receptor SUCNR1 (succinate receptor 1 or GPR91) senses the citric cycle intermediate succinate and is implicated in various pathological conditions such as rheumatoid arthritis, liver fibrosis, or obesity. Here, we describe a novel SUCNR1 antagonist scaffold discovered by high-throughput screening. The poor permeation and absorption properties of the most potent compounds, which were zwitterionic in nature, could be improved by the formation of an internal salt bridge, which helped in shielding the two opposite charges and thus also the high polarity of zwitterions with separated charges. The designed compounds containing such a salt bridge reached high oral bioavailability and oral exposure. We believe that this principle could find a broad interest in the medicinal chemistry field as it can be useful not only for the modulation of properties in zwitterionic compounds but also in acidic or basic compounds with poor permeation.

INTRODUCTION

SUCNR1 (succinate receptor 1, initially named GPR91) is a G-protein-coupled receptor (GPCR), which was orphanized in 2004 by He et al.,¹ identifying succinate as its endogenous ligand.² Succinic acid is a small dicarboxylic acid deprotonated under physiological conditions, thus acting in its anionic form, succinate. While used under the code E363 as a dietary supplement (flavor enhancer and acidifier), it is a crucial citric acid cycle intermediate and therefore an important part of the ATP formation and energy supply of the cell. As such, succinate is normally located in the mitochondria. However, under certain pathological conditions, succinate can be released into the extracellular space and function as a signaling molecule³ that is recognized as a danger signal⁴ by SUCNR1 located on the plasma membrane.

Succinate and SUCNR1 signaling were implicated in local stress conditions including ischemia, hypoxia, toxicity, and hyperglycemia.^{2,5} Moreover, the activation of SUCNR1 by

succinate has been linked to several other pathological conditions such as liver fibrosis,⁶ atherothrombosis,⁷ hypertension,^{8,9} obesity,¹⁰ or retinal vascularization.¹¹ Succinate also plays an important role in inflammation as it serves as an inflammatory signal inducing IL-1 β through HIF1 α stabilization in macrophages.⁴ Furthermore, dendritic cells express high levels of SUCNR1 and succinate proved to be required for dendritic cell trafficking¹² and T_H17 cell expansion.¹³ In arthritis patients, extracellular succinate accumulates in high concentration in the synovial fluid.¹⁴ The importance of

Received: June 15, 2020

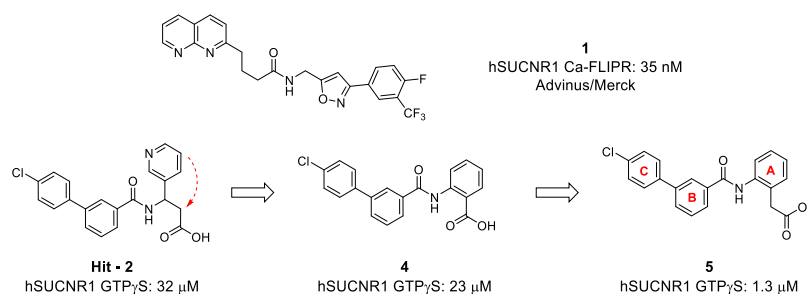


Figure 1. Known SUCNR1 antagonist **1**¹⁶ and HTS hit (**2**) to lead (**5**) optimization.

succinate in this disease could further be demonstrated using SUCNR1-deficient mice that were protected not only from the development of the disease but also from the activation of macrophages and IL-1 β production compared to the wild-type animals.¹⁵ Moreover, SUCNR1-deficient mice demonstrated reduced neutrophil infiltration, lower amounts of proinflammatory cytokines in the joints, and a decreased number of antigen-specific T_H17 cells.¹⁵ Based on these data, SUCNR1 represents an interesting pharmacological target and SUCNR1 antagonists could be useful for the treatment of various diseases. Despite the importance of succinate and its receptor in the pathology of various diseases, so far only one class of SUCNR1 antagonists has been disclosed by the Advinus/Merck group¹⁶ represented by compound **1** (Figure 1). Interestingly, succinate analogs, which act as SUCNR1 agonists, were recently disclosed by two independent groups, demonstrating that succinate seems to bind to SUCNR1 in its cis-conformation.^{17–19} In this article, we describe the discovery and optimization of a novel class of SUCNR1 antagonists for which our group has recently disclosed an X-ray structure resolving their binding into this GPCR.²⁰ While in the previous publication we focused on the structural biology aspects, here, we describe hit-to-lead efforts as well as optimization of the properties in our zwitterionic lead.

RESULTS AND DISCUSSION

To identify novel SUCNR1 antagonists that are structurally different from the known compound series, we performed a high-throughput screening (HTS) campaign using CHEM-1 cells stably expressing human SUCNR1. Out of several interesting hits identified, **2** (JC-59-GF68,²⁰ Figure 1) stood out due to its good drug-like properties,²¹ especially its rather low molecular weight (381 Da), good water solubility (>286 g/L), and low intrinsic clearance (25 μ L/min/mg) in rat liver microsomes. In addition, there was a clear preference for the (*S*)-enantiomer (**3**, 12 μ M, Table 1), while the corresponding (*R*)-enantiomer (not shown) did not inhibit SUCNR1 signaling even at 100 μ M concentration. This enantiodifferentiation indicated real binding into SUCNR1, making the scaffold rather appealing for further investigation.

During early hit optimization, the scaffold could be simplified without losing potency by moving the carboxylate onto the aryl ring while replacing the pyridine by a phenyl ring (**4**). Further homologation of the carboxylate led to phenylacetic acid **5** (PB-20-OV24,²⁰ Figure 1) with almost 20-fold improvement in SUCNR1 inhibition compared to **4** (Table 1). Compared to the original hit **2**, the lead compound **5** also displayed an improved permeability by 1.5 log units as determined by the parallel artificial membrane permeability assay (PAMPA)²² while keeping the lipophilicity in a rather

Table 1. Optimization of the Hit 2

Compd.	Structure	hSUCNR1 ^a GTP γ S [μ M]	logD _{7.4}	logPAMPA ^b [cm/s]
2 JC-59-GF68 ²⁰		32	0.9	-5.3
3		12	1.3	-5.3
4		23	3.0	-3.7
5 PB-20-OV24 ²⁰		1.3	1.9	-3.8
6		1.3	1.4	-3.6
7 NF-58-EJ40 ²⁰		0.025	0.5	-5.5

^aIC₅₀ determined as a mean ($n \geq 3$) in the [³⁵S]GTP γ S assay run with membranes prepared from stably transfected SUCNR1 in human CHEM-1 cells. ^bPermeability determined by high-throughput PAMPA.²²

polar range (log D_{7.4}²³ of 1.9). The addition of a fluorine atom into the *ortho*-position of the amide group on B-ring (for the annotation of the three rings, see Figure 1) was tested for its

possible introduction of a conformational lock²⁴ that could further help in improving the potency. Unfortunately, this proved not to be the case since both the fluorinated analog **6** and nonfluorinated **5** showed the same potency (1.3 μM , Table 1). However, the permeability was slightly enhanced, thus following a known effect of a fluorine atom placed into close proximity of a polar NH such as an amide²⁴ or pyrrole group.²⁵ Counterintuitively, the fluorine atom in **6** also led to decreased lipophilicity (by 0.5 log unit), potentially as a result of an increased dipole moment in such a molecule.^{26,27} This was in line with the calculated dipole moment from quantum chemical calculations being higher for **6** (4.8) than for **5** (3.1). A fruitful modification of the scaffold could be achieved by the introduction of basic amines in the *para*-position of the C-ring because such analogs, as exemplified by **7** (NF-58-EJ40,²⁰ Table 1), inhibited SUCNR1 with high potency. Unfortunately, these derivatives became highly polar and hence poorly permeable.

Due to a pronounced similarity of this scaffold to the complement factor D (FD) inhibitors recently described by our colleagues,²⁸ it became obvious to test some of the *meta*-benzylamine-containing FD inhibitors (**8** and **9**, Table 2) for

Table 2. Selectivity Profile of Selected Analogs against Selected Serine Proteases

Compd.	Structure	hSUCNR1 ^a GTP γ S [μM]	FD ^b [μM]	FXIa ^c [μM]
8		27	0.12	2.8
9		>100	0.008	0.64
10		0.30	>100	5.8

^aIC₅₀ determined as a mean ($n \geq 3$) in the [³⁵S]GTP γ S assay run with membranes prepared from stably transfected SUCNR1 in human CHEM-1 cells. ^bIC₅₀ ($n \geq 2$) determined by the recombinant human complement factor D time-resolved fluorescence resonance energy transfer (TR-FRET) assay. ^cIC₅₀ ($n \geq 2$) determined by the human factor XIa TR-FRET assay.²⁹

their inhibition of SUCNR1. Although beneficial in the *para*-position, as demonstrated by the potency of **7** and its X-ray structure²⁰ showing a direct interaction of the adjacent piperazine nitrogen with E18^{1,31}, the basic amine in the *meta*-position of the C-ring (**8**) proved much less potent (27 μM) compared to **7** (0.025 μM) or even compound **5** (1.3 μM) missing the basic amine (Table 1). A second FD inhibitor, the nonamide analog **9** (Table 2), lost SUCNR1 potency completely (>100 μM), while it was highly potent against FD²⁸ and also factor XIa (FXIa).²⁹ Rather surprisingly,

an additional chlorine atom in the *para*-position in the C-ring of **8** (**10**) could rescue the SUCNR1 potency, whereas it completely prevented binding of such analogs to FD but not to FXIa (Table 2).

The negative effect of the chlorine atom on binding to FD can be explained when analyzing the published X-ray structure of **8** bound to FD (PDB: 6QMT, Figure 2a).²⁸ Whereas the C-ring is nicely filling the S1 pocket of this serine protease and its benzylamine is interacting with Asp189 and Ser190 as well as two water molecules, the Ser190 side chain is rather close to the *para*-position of the C-ring with a distance of 3.4 Å. This indicates that an additional chlorine atom in this position would not be favorable, which was confirmed by docking of a chloro-analog **10** into FD. This study demonstrated that to accommodate the chlorine atom in **10**, the compound had to shift away from Ser190 by roughly 1 Å and, as a consequence, the amine was not able to interact with Asp189 and Ser190 anymore (Figure 2b). Gratifyingly, compound **10** also showed improved potency against SUCNR1 compared to the simple chloro-analog **5**, thus indicating a synergistic effect of these two substituents for inhibition of SUCNR1. The *meta*-benzylamine in FD- and FXIa-inhibitors was shown to be crucial for these serine proteases^{28,29} as it participates in an interaction with an essential aspartate.³⁰ Therefore, our strategy to avoid cross-reactivity with these proteases was to keep the potency-boosting chlorine atom in the *para*-position as well as to probe larger substituents in the *meta*-position varying the position of the basic amine.

Similar to analog **7**, the presence of the amine in compound **10** led to much lower permeability (logPAMPA: -5.3 cm/s) compared to nonamine analog **6** (logPAMPA: -3.6 cm/s, Table 3). The reason for such behavior could be in the zwitterionic nature of such compounds.^{31–33} The carboxylic acid in this scaffold was shown to be essential for binding to SUCNR1 as it makes several interactions with the receptor: Tyr26^{1,39}, Tyr79^{2,64}, and Arg276^{7,39} residues (Figure 3).²⁰ Arg276^{7,39} (Arg281^{7,39} in human SUCNR1) is one of the four amino acids implicated in the binding of succinate by SUCNR1¹, which illustrates the importance of the carboxylic acid group in these antagonists. The amine could potentially be omitted to avoid the amphiphilicity of these inhibitors; however, its presence not only helped in increasing the potency (**10** vs **5**, Table 2) but the zwitterionic nature of the compounds also had a positive effect on plasma protein binding (PPB). Whereas the single ionic compound **5** was bound tightly (>99%) to the human plasma, its zwitterionic analog **10** displayed a reduced human PPB of 97.9%. Since the free drug concentration is crucial for the action of a bioactive compound,³⁴ we wished to keep the zwitterionic nature of this class of SUCNR1 inhibitors. Despite options to improve the permeability and bioavailability of zwitterions by formulations, e.g., using salts or delivery systems,³⁵ we preferred to explore possibilities for the improvement of the intrinsic properties rather than to rely on such efforts.

As previously observed,²⁸ the two close analogs **8** and **9** differ significantly in their permeability and oral bioavailability despite showing similar clearance in mice (Table 3). This is really interesting, especially because also the pK_a values³⁶ for both compounds were measured to be rather similar (4.4 and 9.4 for **9**; 4.0 and 9.5 for **8**), indicating that at neutral pH both of them should be doubly charged (zwitterionic) and hence poorly permeable.³⁷ Nevertheless, **9** with the methyleneoxy linker was fully absorbed in mice, whereas the bioavailability of

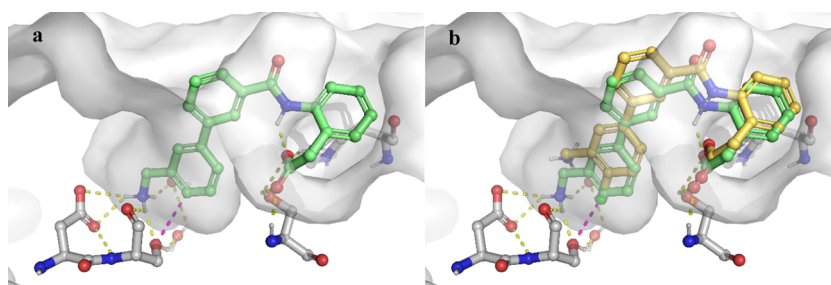


Figure 2. (a) Crystal structure of **8** in complex with factor D (PDB: 6QMT).²⁸ The protein is in surface representation, the ligand as well as amino acids/water involved in polar interactions with the ligand are shown as sticks. Yellow: polar interactions between the compound and the protein. Magenta: the distance between the phenyl carbon of **8** in the *para*-position to Ser190 side chain equals 3.4 Å. (b) **10** (yellow sticks) docked in factor D cavity (6QMT)²⁸ superimposed on the co-crystal structure of **8** (green).

Table 3. ADME Properties of Selected Compounds

Compd.	Structure	logPAMPA ^a [cm/s]	F ^b [%]	AUC po dn ^c [nmol.h/L]	Cl ^d [mL/min/kg]
6		-3.6	95	7814	10
8		<-5.3	10 ^e	206 ^e	22
9		-4.5	>100 ^e	3646 ^f	14

^aPermeability determined by high-throughput PAMPA.²² ^bOral bioavailability calculated as the dose-normalized ratio of extravascular AUCextrap to IV AUCextrap; both parameters were determined as a mean of 3 animals (male C57BL/6 mice). ^cExposure (AUC; dn = dose-normalized to 1 mg/kg) measured as a mean of three animals (male C57BL/6 mice) after po dosing (3 mg/kg) using MC:Water:Tween80 (0.5:99:0.5) formulation. ^dClearance measured as a mean of three animals (male C57BL/6 mice) after iv dosing (1 mg/kg) using an NMP:plasma (10:90) formulation. ^eF and AUC po dn determined in three animals (male C57BL/6 mice) after po dosing (10 mg/kg) using 30% PEG300, 50% of (20% Cremophor EL), and a PBS formulation.²⁸ ^fF and AUC po dn determined in three animals (male C57BL/6 mice) after po dosing (10 mg/kg) using an MC:water:Tween80 (0.5:99.4:0.1) formulation.²⁸

its amide analog **8** was only 10% (Table 3). This comparison could suggest that the amide might be responsible for these unfavorable properties, a well-known phenomenon in peptides.³⁸ However, the good oral absorption of non-zwitterionic amide **6**, again with a comparable clearance to **8** (Table 3), demonstrated that the poor permeability and bioavailability of **8** was not necessarily caused by the amide group alone but rather by a combination of amide and the zwitterion. Whereas the amide was not required for binding of this scaffold to FD and could therefore be replaced by the methyleneoxy linker, in our case, the amide carbonyl was needed for a water-mediated interaction with His99^{3,33} residue

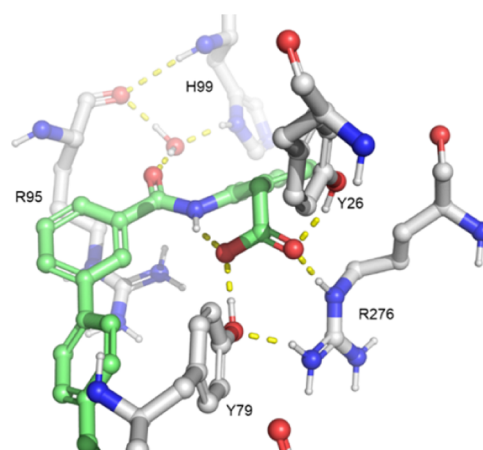


Figure 3. Key interactions of amide carbonyl and carboxylate in **7** with SUCNR1 (PDB: 6RNK).²⁰

as well as the Arg95^{3,29} backbone carbonyl of SUCNR1²⁰ (Figure 3). In human SUCNR1, these amino acids (Arg99^{3,29} and His103^{3,33}) were shown to be required for the binding of its endogenous ligand succinate.¹ Therefore, the amide replacement by methyleneoxy linker (**9**) resulted in a complete loss of potency against SUCNR1 (Table 2).

Being puzzled by such a significant difference in the permeability and oral absorption of the zwitterions **9** and **10**, low molecular weight X-ray structures of both compounds (as HCl salts) were generated (Figure 4), which revealed a substantial difference in the conformations of the two closely related analogs. While **10** showed an HCl-mediated interaction of the amine with the acid moiety, **9** displayed a charge-assisted hydrogen bond between these two functional groups, which corresponds to the formation of a salt bridge in the aqueous phase. Intramolecular salt bridges as electrostatic interactions are known to contribute to peptide stabilization, protein folding, flexibility, and function.³⁹ Similar to the effect of intramolecular hydrogen bonds,⁴⁰ we speculated that the presence of the intramolecular salt bridge in **9** could explain its superior permeation and absorption properties because it would allow for significant shielding of the polarity of the two charged groups. Apparently, the formation of the intramolecular salt bridge was feasible in **9** thanks to a greater flexibility of the methyleneoxy linker, whereas in **10**, the salt bridge seemed to be prevented by the rigid amide bond. In addition, even the HCl-mediated interaction in **10** did not seem optimal (Figure 4). To get engaged in such an interaction (HCl-mediated), the A-ring got significantly twisted (60°)

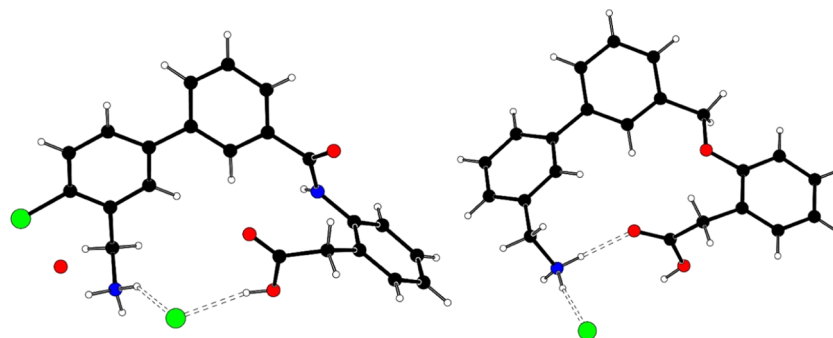


Figure 4. Structure of the hydrochlorides of **10** (left) and **9** (right) in the crystal. Hydrogen bonds are shown as dotted lines.

toward the amide bond,⁴¹ whereas the biaryl group was unusually bent (10°)⁴² and the two phenyl rings displayed a somewhat lower torsion angle than usual (24°). Of course, such a conformation could also be caused by crystal packing; nevertheless, it clearly demonstrated that the rigidity of the amide group made it difficult in **10** to bring the two charged groups into close proximity of 4 Å as required for a productive electrostatic interaction.³⁹

Based on these observations, we decided to explore the feasibility of salt bridge formation within the amide scaffold to study whether such an intramolecular salt bridge could rescue the poor permeability and absorption properties of the amide zwitterions. We envisaged to investigate different types of amines attached to a *meta*-alkoxy group. Gratifyingly, the simplest analog **11** retained SUCNR1 potency, although permeability was not changed (Table 4).

Interestingly, conformationally restricted amines such as azetidine (**12**), pyrrolidine (**13**), and the two possible piperidine isomers (**14** and **15**) showed similar potency as the flexible amine **11**, indicating that the amino-substituent was devoid of any crucial interaction with the receptor. With respect to permeability, these derivatives also did not show any improvement, except for **15** (Table 4). With only a marginal change in the structure compared to the 4-piperidyl analog **14**, but also to pyrrolidine **13**, the 3-piperidyl compound **15** demonstrated quite a remarkable increase (1 log unit) in permeability as well as lipophilicity (Table 4). Based on compound **9**, this improvement was interpreted by a successful formation of an intramolecular salt bridge being mediated by the 3-piperidyloxy substituent but not by any other substituent tried. Apparently, this particular substituent allowed for the right geometry and distance to bring the two charged groups in this scaffold into close proximity (<4 Å).³⁹ As a consequence, the intramolecular salt bridge may be responsible for shielding of the charges, similar to an intramolecular hydrogen bond,⁴³ and the compound may appear as much less polar and hence more permeable than analogs with separated charges. Another hint for the existence of the salt bridge in **15** arose from the ionic profile for the two piperidine isomers. The pK_a values for the acid and base of 4-piperidine analog **14** were determined to be 4.1 and 9.9, respectively, being virtually the same as for 3-piperidine **15** (4.1 and 9.4). For this reason, both compounds were expected to be in the zwitterionic form at neutral pH and, as such, to display similar permeation properties. This was clearly not the case, as evidenced by the observed $\log D$ and permeability data for these two analogs. We concluded that to explain the difference in permeability for these two analogs, **15** must have displayed a different conformational behavior compared to **14**, allowing for

Table 4. Optimization toward the Formation of a Salt Bridge for Improved Permeability

Compd.	Structure	hSUCNR1 ^a GTP γ S [μ M]	$\log D_{7.4}$	$\log P_{\text{AMPA}}^b$ [cm/s]
10		0.30	2.1	-5.3
11		0.27	2.8	-5.4
12		0.14	2.6	-5.2
13		0.14	2.8	-5.3
14		0.14	2.5	-5.4
15		0.52	3.6	-4.4

^aIC₅₀ determined as a mean ($n \geq 3$) in the [³⁵S]GTP γ S assay run with membranes prepared from stably transfected SUCNR1 in human CHEM-1 cells. ^bPermeability determined by high-throughput PAMPA.²²

shielding of the two opposite charges. Applying an in-house-developed quantum chemical workflow (ReSCoSS, described elsewhere)⁴⁴ for the elucidation of conformational behavior

and associated changes in polarity revealed that **14** and **15** populated remarkably different shapes in aqueous solution (Figure 5). While **14** preferred an elongated conformation, **15**

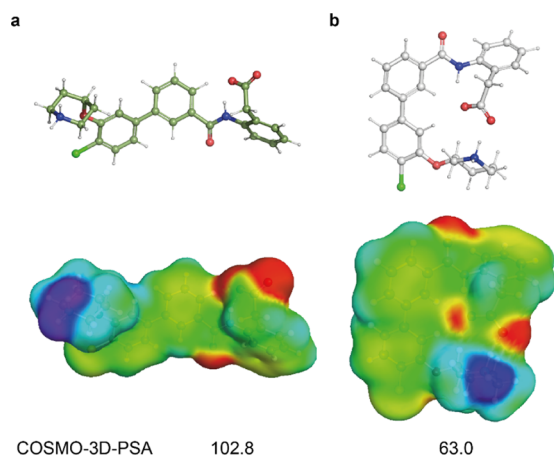


Figure 5. Minimum-energy conformation in water at the TZVPD-FINE19 level for (a) **14** and (b) **15** (first row) and associated σ -surfaces (second row). The (*R*)-enantiomer was modeled for **15**. The folded conformation observed for **15** with the intramolecular salt bridge leads to a drastic reduction in the overall polar surface area as quantified by COSMO-3D-PSA.⁴⁴

was predominantly folded with an intramolecular salt bridge formed between the piperidyl moiety and the carboxylic acid moieties. Comparing the polar surface areas derived from the electrostatic surfaces of these two different structures (COSMO-3D-PSA)⁴⁴ as well as visual inspection of these surfaces revealed that the salt bridge in **15** dramatically reduces the polarity of both charged moieties. Even taking into account that the permeating species may or may not correspond to the minimum-energy conformer in water, the reduction of the polar surface area observed here seems causative in allowing for better permeation.

After the successful identification of a suitable substituent forming the internal salt bridge in the zwitterionic amide scaffold, the stereochemistry of chiral 3-oxopiperidine was investigated for potency and physicochemical properties. Surprisingly, both enantiomers were found to be equally potent, even with similar properties, except for PPB. For unknown reasons, PPB was measured to be lower for the *R*-enantiomer as exemplified by **16** (Table 5) showing human PPB of 96.0% and mouse PPB of 97.4%, while the binding of its (*S*)-enantiomer (not shown) to human plasma was 98.6% and mouse plasma 99.7%. Therefore, the (*R*)-enantiomer was preferred for further exploration (Table 5). Adding a fluorine atom into the B-ring (**16**) or C-ring (**17**) led to slightly improved potency compared to **15**. Both compounds displayed good bioavailability and oral exposure in mice, which supported our internal salt bridge hypothesis. The addition of a second fluorine atom into the A-ring (*para* to the anilide-NH) of **17** resulted in a metabolically more stable derivative **18**, which led to a further significant (10-fold) improvement in oral exposure compared to **17** (Table 5). Moving the fluoro-substituent in the C-ring from the *ortho*- to the *para*-position to the alkoxy substituent (**19**) caused an increase in clearance, leading to diminished oral exposure despite reaching full bioavailability. The addition of another fluorine atom into the B-ring resulted in compound **20** with very low clearance while

keeping good permeability and oral bioavailability. As a consequence, **20** reached a very high oral exposure of 37 000 nmol·h/L (Table 5). Interestingly, the SUCNR1 potency was not much influenced by these modifications.

To confirm the presence of the intramolecular salt bridge, a low molecular weight X-ray structure of compound **20** was generated (Figure 6). This structure confirmed our hypothesis, i.e., 3-piperidyl is capable of participating in an internal salt bridge with the carboxylate since the piperidine nitrogen was within a favorable distance of 3.1 Å to the carboxylate oxygen. In addition, compared to the X-ray structure of the analog **10**, the structure of **20** seemed closer to the expected minimum conformation with ring A twisted by 42° toward the amide bond, the biaryl group not being bent anymore, and the two phenyl rings displaying a rather normal torsion angle of 54°.

Unfortunately, a poor species cross-reactivity was observed for this scaffold, as the advanced inhibitors displayed virtually no inhibition of rat and mouse SUCNR1. For example, compound **20** showed only 23% inhibition of mouse and 56% of rat SUCNR1 activity at 100 μM concentration, whereas IC₅₀ on human SUCNR1 was 88 nM. Due to this drawback, these compounds could not be tested in any of the rodent models of arthritis or any other diseases. To understand the species difference, an X-ray structure of **20** bound to SUCNR1 was solved (Figure 7a), using a humanized rat construct recently disclosed by our group.²⁰ As already described,²⁰ the rat SUCNR1 proved to be more suitable for crystallization due to the lack of glycosylation sites as well as higher biochemical stability than human SUCNR1. Mutagenesis studies identified a rat SUCNR1 double mutant (K18E, K269N) that allowed for binding of human selective SUCNR1 inhibitor **7**, thus indicating the key residues responsible for the species selectivity.²⁰ Strikingly, the residues of the required two mutations are of a very different polarity, especially the mutation of K18 in rats into an oppositely charged glutamate found in human SUCNR1. While the inhibitor **20** does not make any direct interaction with E18 or N269 in the X-ray structure (Figure 7a, in gray), in the case of E18, this may actually happen in solution since the highest-scoring predicted pose from docking (Figure 7a, in green) forecasts a salt bridge interaction between the piperidine moiety of the ligand and E18 by virtue of a simple rotation around the biaryl axis. Even more strikingly, the two amino acid mutations (K18E and K269N), i.e. away from lysines, decreased the positive formal charge present in the binding site of the rat receptor. This is clearly reflected in a marked change in electrostatics in the binding site (Figure 7b,c), allowing the positively charged piperidine moiety to be accommodated in the humanized receptor.

Remarkably, this class of inhibitors embodied by **20** displays a chameleonic nature,⁴⁵ with the extended conformation binding to the receptor (Figure 7), while the closed conformation with an intramolecular salt bridge seems to be favorable in aqueous solution (quantum chemical studies, Figure 5) as well as in the solid state for the isolated compound (low-molecular-weight crystal structure, Figure 6). The coexistence of the two classes of conformations that are decidedly different in polarity⁴⁶ in structures like **20** likely allows transport across membranes during absorption in the closed conformation, while these groups may be released when binding to the target. We believe that this intriguing characteristic of the zwitterions described in this publication will find wider application in medicinal chemistry, especially in

Table 5. Optimization of Piperidine-Based Intramolecular Zwitterion

Compd.	Structure	hSUCNR1 ^a GTPγS [μM]	logPAMPA ^b [cm/s]	F ^c [%]	AUC po dn ^d [nmol.h/L]	Cl ^e [mL/min/kg]
16		0.19	-5.3	46 ± 3	1437 ± 93	11 ± 1
17		0.076	-5.0	81 ± 4	2353 ± 120	12 ± 2
18		0.092	-4.9	93 ± 11	26100 ± 2950	1.2 ± 0.2
19		0.090	-4.4	137 ± 46	5737 ± 1931	8.0
20		0.088	-5.1	74 ± 14	37000 ± 6533	0.6 ± 0.1

^aIC₅₀ determined as a mean ($n \geq 3$) in the [³⁵S]GTPγS assay run with membranes prepared from stably transfected SUCNR1 in human CHEM-1 cells. ^bPermeability determined by high-throughput PAMPA.²² ^cOral bioavailability ± SD calculated as the dose-normalized ratio of extravascular AUC_{extrap} to IV AUC_{extrap}; both parameters were determined as a mean of three animals (male C57BL/6 mice). ^dExposure (AUC; dn = dose-normalized to 1 mg/kg) ± SD reported in nM·h and measured as a mean of three animals (male C57BL/6 mice) after po dosing (3 mg/kg) using an MC:water:Tween80 (0.5:99:0.5) formulation. ^eClearance measured as a mean ± SD of three animals (male C57BL/6 mice) after iv dosing (1 mg/kg) using an NMP:plasma (10:90) formulation.

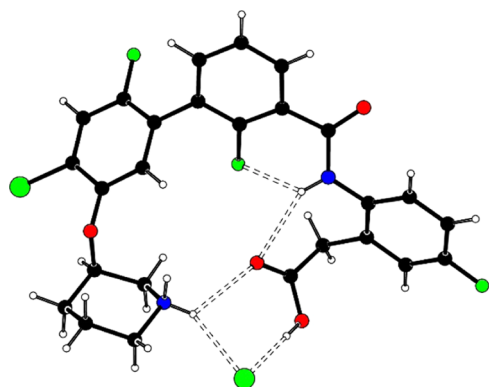


Figure 6. Structure of the hydrochloride of compound 20 in the crystal. Hydrogen bonds are shown as dotted lines.

the design of new bioactive molecules containing basic or acidic groups and lacking good permeability and/or oral absorption properties.

CHEMISTRY

The majority of compounds described in this publication were prepared by a convergent route using a coupling of amide building blocks with simple or complex C-rings (Scheme 3). Whereas the amide building blocks 21 and 22 were made by a direct acylation of the commercially available methyl 2-(2-aminophenyl)acetate with corresponding benzoic acid chlorides, their analogs 25 and 26 required an access to 2-(2-amino-5-fluorophenyl)acetic acid (Scheme 1). This intermediate could be reached from 5-fluorooxindole by opening the lactam upon its heating with 10% aqueous NaOH⁴⁷ and was subsequently acylated with benzoic acid chlorides to provide the corresponding amide acids 23 and 24 in good yields (Scheme 1). These acids were then converted into corresponding methyl esters 25 and 26, and all bromine intermediates were then transformed into boronates (27–30) (Scheme 1).

The C-ring building blocks were rather diverse (Scheme 2). Whereas intermediate 31 could be made by Boc-introduction into corresponding commercial benzylamine, the alkyloxy derivatives (32–rac-36) were prepared by alkylation of

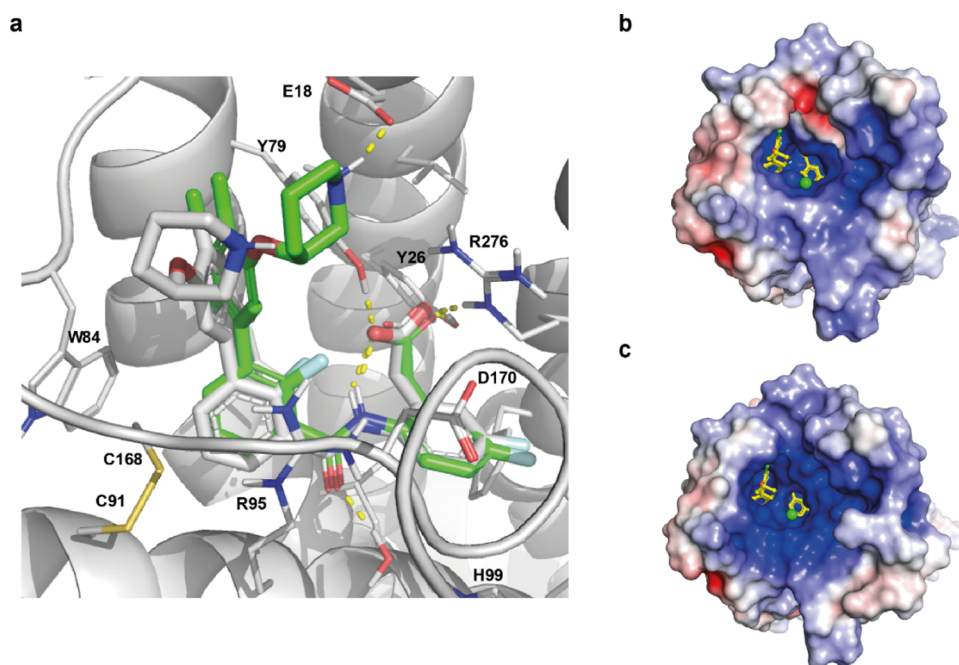
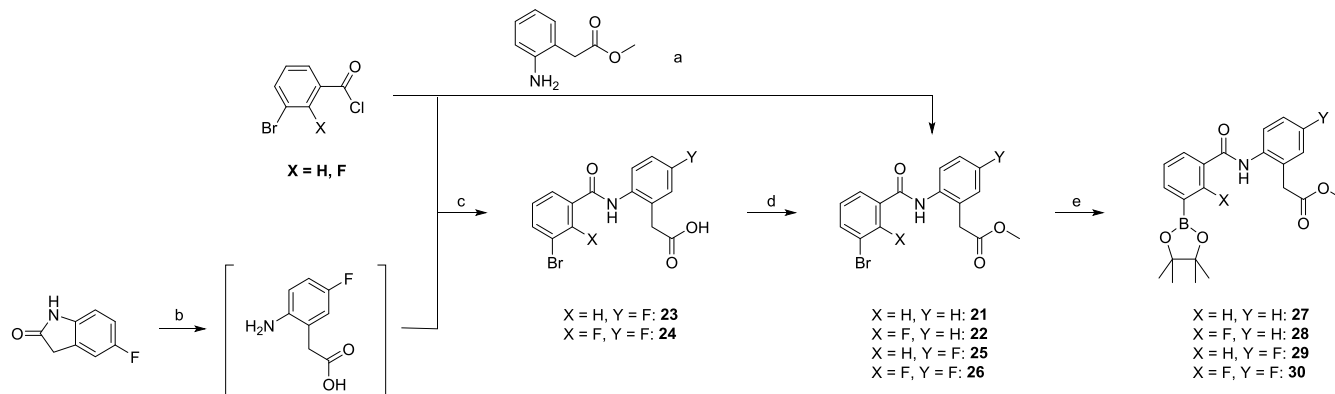


Figure 7. (a) X-ray crystal structure of **20** (grey carbons) bound to humanized rat SUCNR1 (PDB: 6Z10) overlaid onto the top-scoring binding pose from docking (green carbons) forming salt bridge interaction with Glu18. (b) Electrostatic potential mapped onto the molecular surface for humanized rat SUCNR1 and (c) for wild-type rat SUCNR1 (model based on PDB: 6Z10) showing a large concentration of positively charged amino acid residues flanking the binding site. Calculations were done using the APBS plugin in PyMOL.

Scheme 1. Preparation of Amide Building Blocks^a



^aReagents and conditions: (a) Et₃N or *N,N*-diisopropylethylamine (DIPEA), CH₂Cl₂, 23 °C, 1 h (89–97%); (b) 10% NaOH (aq.), 100 °C, 16 h; (c) THF/H₂O, 23 °C, 16 h (76–92% over 2 steps); (d) MeOH, HCl, 23 °C, 16 h (86–98%); (e) (PinB)₂, PdCl₂dppf, KOAc, dioxane, 110 °C, 2 h (62–94%).

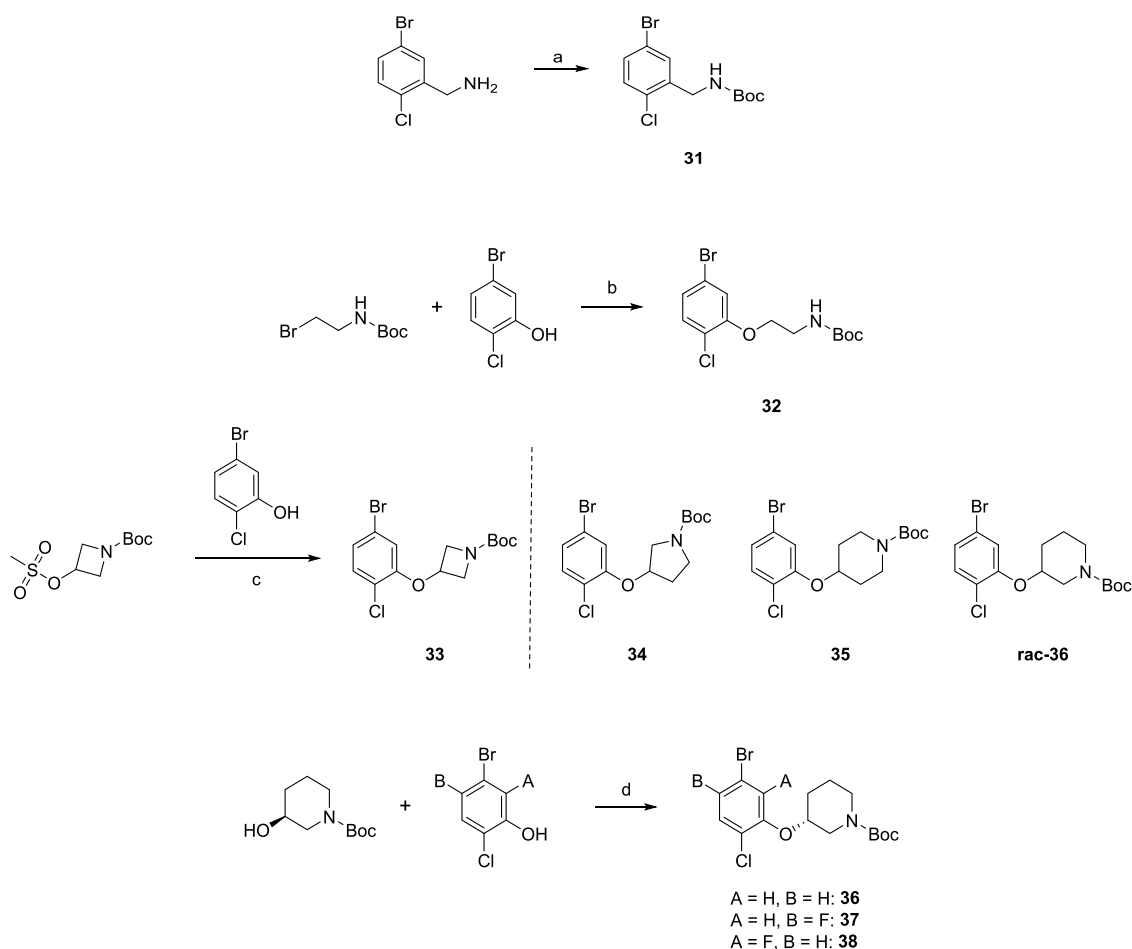
5-bromo-2-chlorophenol. For acyclic alkoxy intermediate **32**, Boc-2-bromoethylamine was used, while for the cyclic substituents, the appropriate mesylates were employed (Scheme 2). In contrast, the enantiomerically pure (*R*)-3-piperidyloxy building blocks (**36–38**) were accessed by the Mitsunobu reaction⁴⁸ of the (*S*)-*N*-Boc-3-piperidinol and various phenols (Scheme 2).

The assembly of different final products is summarized in Scheme 3. Compound **4** was made by saponification of compound **39**, which was prepared from 4'-chloro-[1,1'-biphenyl]-3-carboxylic acid by its activation into acyl chloride and reaction with methyl 2-aminobenzoate. Derivative **6** was synthesized by Suzuki coupling of **22** with *p*-chlorophenyl boronate, whereas compound **10** was accessed from the boron ester **27** and bromo-building block **31** followed by ester

hydrolysis and Boc-cleavage in **40** (Scheme 3). Derivatives possessing diverse alkoxy-substituents (**11–15**) were made by Suzuki coupling of boronate **27** and alkoxy-phenyl bromides **32–rac-36** followed by Boc-cleavage of the resulting acids **41–45** (Scheme 3). In analogy, the enantiomerically pure piperidyloxy analogs **16–20** were prepared via the corresponding acid intermediates **46–50**.

CONCLUSIONS

In this paper, we described the discovery and optimization of a new SUCNR1 antagonist scaffold. Starting from an HTS hit **2** (32 μM), the scaffold could be optimized to SUCNR1 antagonists with high potency such as, e.g. **7** (25 nM). However, the new inhibitors displayed poor permeability and oral absorption, possibly as a result of their zwitterionic nature

Scheme 2. Preparation of C-Ring Building Blocks^a

^aReagents and conditions: (a) Boc_2O , DIPEA, CH_2Cl_2 , 23 °C, 16 h (83%); (b) Cs_2CO_3 , DMF, 120 °C, 6 h (91%); (c) Cs_2CO_3 , DMF, 80 °C, 16 h (16–72%); (d) Ph_3P , diisopropyl azodicarboxylate (DIAD), THF, 60 °C, 16 h (42–77%).

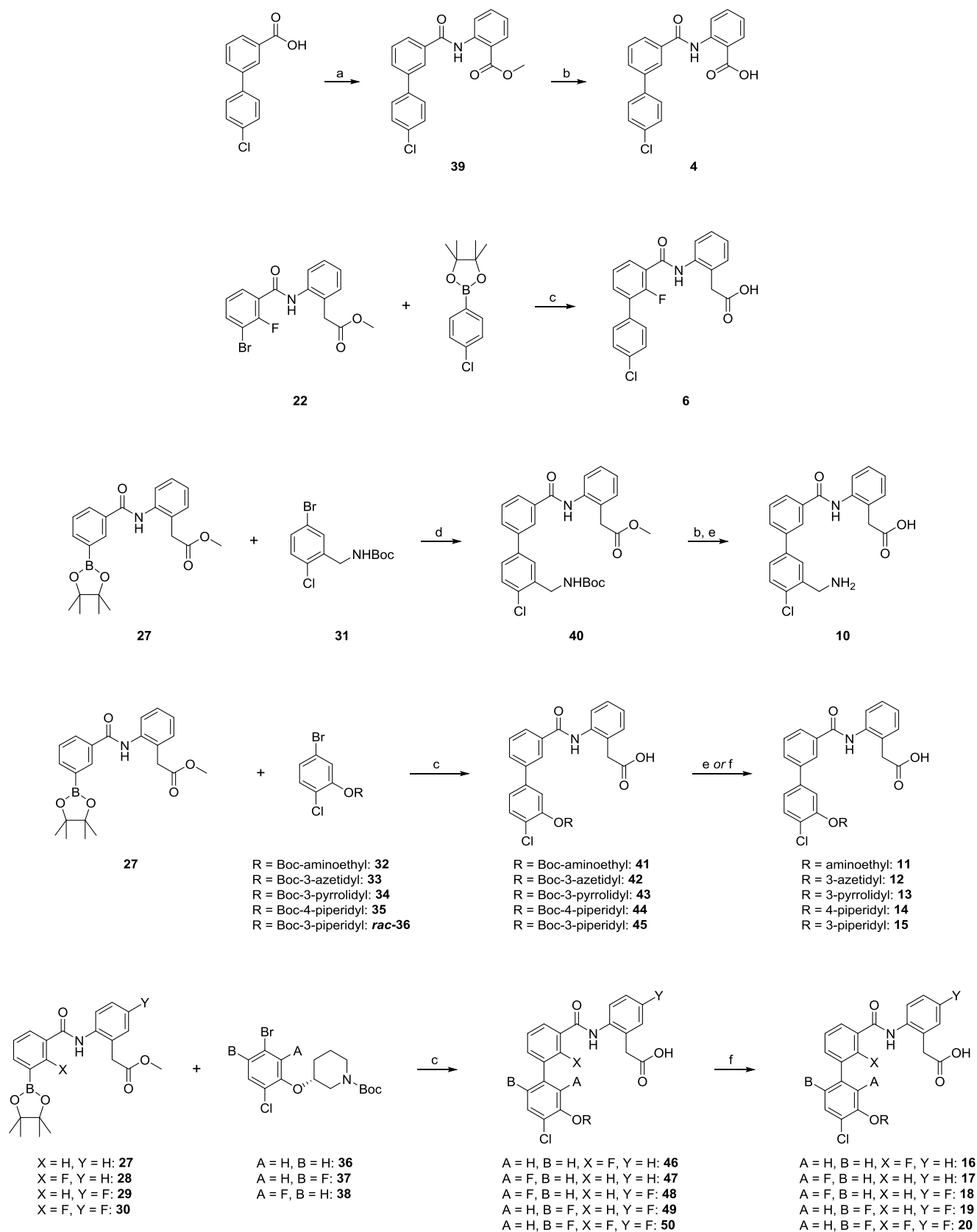
due to the presence of the essential acid group and amine required for potency and favorable properties. As demonstrated by the pair of two closely related zwitterions **8** and **9** with very different absorption properties, the issue for poor permeability and absorption could be caused by the separation of the two adjacent, inversely charged groups as hypothesized from the X-ray structures of **8** and **9**. Whereas the flexible methyleneoxy linker in the well-absorbed compound **9** allowed for a salt bridge formation, its poorly permeable and bioavailable analog **8** contained a rigid amide linker that prevented the salt bridge formation. Since the amide makes key interactions with SUCNR1, a search for suitable amines was performed that would allow for the formation of the salt bridge also in the amide subseries. This effort led to the identification of the 3-piperidyloxy substituent in the C-ring that favored the salt bridge formation as confirmed by the X-ray structure of **20**. According to our hypothesis, the formation of the internal salt bridge provided derivatives with much improved oral absorption. For example, the optimized analog **20** displayed nearly full bioavailability and a very high oral exposure in mice ($37 \mu\text{mol}\cdot\text{h}/\text{L}$), also achieved thanks to its very low clearance ($0.6 \text{ mL}/\text{min}/\text{kg}$). Finally, the X-ray structure of **20** bound to SUCNR1 demonstrated an excellent property of such zwitterions, namely, their coexistence in two different conformations. While the closed conformation is forced by the salt bridge and may play an important role during

permeation, it allows for the breaking of the salt bridge, leading to the stretched conformation required by the receptor. We believe that this work allows for the further development of SUCNR1 inhibitors, thanks to the presented SAR and disclosure of the second X-ray structure of an antagonist bound to SUCNR1. In addition, this work might also find a wide interest in the medicinal chemistry community as it describes the design of zwitterions with an internal salt bridge that can be highly useful for the improvement of permeability and/or oral absorption of new bioactive compounds containing basic or acidic groups.

EXPERIMENTAL SECTION

Chemistry. All reagents and solvents were purchased from commercial suppliers and used without further purification. All reactions were performed under inert conditions (argon) unless otherwise stated. NMR spectra were recorded on a Bruker 400 MHz NMR spectrometer. Chemical shifts are reported in parts per million (ppm) relative to an internal solvent reference. Significant peaks are tabulated in the order of multiplicity (s, singlet; d, doublet; t, triplet; q, quartet; quintet; m, multiplet; br, broad), coupling constants, and the number of protons. Final compounds were purified to $\geq 95\%$ purity as assessed by analytical liquid chromatography:

LCMS method a. Waters UPLC Acquity; column: CORTECS C18 + 2.7 μm , 2.1 mm \times 50 mm at 80 °C, eluent A: water + 4.76% isopropanol + 0.05% HCOOH + 3.75 mM NH_4OAc , B: isopropanol

Scheme 3. Preparation of the Final Products^a

^aReagents and conditions: (a) (COCl)₂, DMF (cat.), CH₂Cl₂, 23 °C, 2 h, then methyl 2-aminobenzoate, Et₃N, CH₂Cl₂, 23 °C, 20 h (86%); (b) LiOH, H₂O, MeOH, 50 °C, 3–18 h (45–89%); (c) Pd(PPh₃)₄, NaHCO₃, DME/H₂O, 80 °C, 16 h (50–92%); (d) PdCl₂dppf, Na₂CO₃, DMF/H₂O, 80 °C, 0.5 h (87%); (e) TFA, CH₂Cl₂, 23 °C, 4 h (57% over 2 steps); (f) HCl, dioxane/CH₂Cl₂, 23 °C, 16 h (53–95%).

+ 0.05% HCOOH, gradient: 1–50% B in 1.4 min, 50–98% in 0.3 min. Flow: 1.0 mL/min.

LCMS method b. Waters UPLC Acquity; column: BEH C18 1.7 μm , 2.1 mm \times 100 mm at 80 °C, eluent A: water + 4.76% isopropanol + 0.05% HCOOH + 3.75 mM NH_4OAc , B: isopropanol + 0.05% HCOOH, gradient: 1–60% B in 8.4 min, 60–98% in 1.0 min. Flow: 0.4 mL/min.

The preparation of compounds **2**, **5**, **7**, **8**, and **9** has been previously described.^{20,28} Compound **3** was prepared according to the procedure described for compound **2**,²⁰ using the commercially available (*S*)-3-amino-3-(pyridin-3-yl)propanoic acid (Chem-Impex).

Preparation of Boronic Esters. A mixture of bromo-compound (**1** equiv), bis(pinacolato)diboron (**1.1** equiv), and KOAc (**2** equiv) in dioxane (**0.2** M concentration) was degassed with argon. After the addition of $\text{PdCl}_2\text{dppf}\cdot\text{CH}_2\text{Cl}_2$ (**0.1** equiv), the reaction mixture was heated at 110 °C for 2 h. After being cooled to 23 °C, the reaction mixture was filtered through Celite and washed with EtOAc. The reaction mixture was then treated with water, the aqueous layer was extracted with EtOAc, and the combined organic layers were dried (Na_2SO_4) and concentrated. The residue was purified by column chromatography to provide the boronates.

Phenol Alkylation by Mesylates. A mixture of 5-bromo-2-chlorophenol (**1** equiv), mesylate (**1** equiv), and Cs_2CO_3 (**1.1** equiv) in DMF (**0.05** M concentration) was stirred at 80 °C for 16 h. After being cooled to 23 °C, the reaction mixture was diluted with ether and washed with water and brine, dried (Na_2SO_4) and concentrated. The crude product was purified by column chromatography to provide the phenylalkyl ethers.

Phenol Alkylation by the Mitsunobu Reaction. (*S*)-1-*N*-Boc-3-hydroxypiperidine (**1** equiv) was added at 23 °C to a mixture of phenol (**1** equiv), DIAD (**1.5** equiv) and PPh_3 (**1.5** equiv), in THF (**0.1** M concentration), and the resulting solution was stirred at 23 °C for 16 h. The reaction mixture was concentrated and purified by column chromatography to provide phenylalkyl ethers.

Suzuki Coupling. A mixture of the bromo intermediate (**1** equiv), boronate (**1** equiv), and saturated NaHCO_3 (**5** equiv) in DME/water (**4:1**, **0.04** M concentration) was degassed with argon. $\text{Pd}(\text{PPh}_3)_4$ (**0.03** equiv) was then added, and the mixture was heated at 80 °C for 16 h. After being cooled to 23 °C, the beige suspension was diluted with **0.2** M HCl and extracted with ethyl acetate. The organic layers were washed with water and brine, dried (Na_2SO_4), and concentrated. The crude material was purified by column chromatography to provide the coupling products.

Boc-Cleavage with HCl. HCl (**4** M) in dioxane (**10** equiv) was added at 0 °C to a solution of Boc-intermediate (**1** equiv) in CH_2Cl_2 (**0.05** M concentration). After being stirred at 23 °C for 16 h, the formed suspension was diluted with ether and the solid was filtered off, washed with ether, and dried in high vacuum to provide the amine products as HCl salts.

Methyl 2-(2-(3-Bromobenzamido)phenyl)acetate (21). A solution of 3-bromobenzoylchlorid (**18.0** g, **82** mmol) in CH_2Cl_2 (**20** mL) was added dropwise at 23 °C to a solution of methyl 2-(2-aminophenyl)acetate (**15.2** g, **82** mmol) and Et_3N (**13.7** mL, **98** mmol) in CH_2Cl_2 (**400** mL). After being stirred at 23 °C for 1 h, the reaction mixture was concentrated and the residue was treated with *t*-BuOMe and stirred at 23 °C for 16 h. The mixture was then cooled to 0 °C, and the solid was filtered off and washed with *n*-hexane. The filtrate was concentrated to 25% of the volume, and the suspension was filtered off again and washed with *n*-hexane. Collected solids were dried in high vacuum to provide the title product as a colorless solid in **25.6** g (**89%**) yield. ^1H NMR (400 MHz, $\text{DMSO}-d_6$, δ) 10.09 (s, 1H), 8.09 (t, $J = 1.8$ Hz, 1H), 7.92 (dt, $J = 7.8$, 1.2 Hz, 1H), 7.80 (ddd, $J = 8.0$, 2.1, 1.0 Hz, 1H), 7.51 (t, $J = 7.9$ Hz, 1H), 7.40–7.29 (m, 3H), 7.25 (td, $J = 7.3$, 1.7 Hz, 1H), 3.74 (s, 2H), 3.52 (s, 3H). ^{13}C NMR (101 MHz, $\text{DMSO}-d_6$, δ) 171.4, 164.0, 136.6, 136.3, 134.3, 131.0, 130.9, 130.7, 130.3, 127.5, 126.9, 126.7, 126.3, 121.6, 51.6, 37.2. LCMS (method a) m/z : 349.9 $[\text{M} + \text{H}]^+$, $t_{\text{R}} = 0.98$ min.

Methyl 2-(2-(3-Bromo-2-fluorobenzamido)phenyl)acetate (22). A solution of 3-bromo-2-fluorobenzoyl chloride (**3.0** g, **12.65** mmol) in CH_2Cl_2 (**10** mL) was added dropwise at 23 °C to a solution of

methyl 2-(2-aminophenyl)acetate (**1.9** g, **11.5** mmol) and DIPEA (**4.1** mL, **23** mmol) in CH_2Cl_2 (**30** mL). After being stirred at 23 °C for 1 h, the reaction mixture was treated with CH_2Cl_2 and 10% NaHCO_3 (aq.). The water phase was extracted with CH_2Cl_2 , and the organic layers were washed with water and brine, dried (Na_2SO_4), and concentrated. The crude product was purified by column chromatography (0–25% ethyl acetate in cyclohexane) to provide the title product as a yellowish solid in **4.1** g (**97%**) yield. ^1H NMR (400 MHz, $\text{DMSO}-d_6$, δ) 10.06 (s, 1H), 7.88 (ddd, $J = 8.2$, 6.7, 1.8 Hz, 1H), 7.66 (ddd, $J = 7.9$, 6.3, 1.7 Hz, 1H), 7.45 (d, $J = 8.0$ Hz, 1H), 7.38–7.19 (m, 4H), 3.77 (s, 2H), 3.59 (s, 3H). ^{13}C NMR (101 MHz, $\text{DMSO}-d_6$, δ) 171.2, 161.9, 155.2 (d, $J = 249.3$ Hz), 135.9, 135.5, 131.1, 123.0, 129.4 (d, $J = 2.0$ Hz), 127.5, 126.3, 126.2, 125.99, 125.97 (d, $J = 13.1$ Hz), 108.9 (d, $J = 21.5$ Hz), 51.6, 36.8. ^{19}F NMR (376 MHz, $\text{DMSO}-d_6$, δ) –108.9. LCMS (method a) m/z : 366.0 $[\text{M} + \text{H}]^+$, $t_{\text{R}} = 0.99$ min.

2-(2-(3-Bromobenzamido)-5-fluorophenyl)acetic Acid (23). 5-Fluoroindolin-2-one (**5.0** g, **33.1** mmol) was dissolved in 10% NaOH (aq.) (**45** mL) and the mixture was stirred at 100 °C for 16 h. After being cooled to 23 °C, concentrated HCl (**8.5** mL) was added and a half of the volume of this mixture was treated at 23 °C with the solution of 3-bromobenzoyl chloride (**2.92** g, **13.3** mmol) in THF (**10** mL) and the reaction mixture was stirred at 23 °C for 16 h. The solid was filtered off, washed with water, and dried in high vacuum to provide the title product as a brown solid in **4.25** g (**76%**) yield. ^1H NMR (400 MHz, $\text{DMSO}-d_6$, δ) 12.33 (s, 1H), 10.14 (s, 1H), 8.10 (t, $J = 1.9$ Hz, 1H), 7.92 (dt, $J = 7.8$, 1.4 Hz, 1H), 7.80 (ddd, $J = 8.0$, 2.1, 1.0 Hz, 1H), 7.50 (t, $J = 7.9$ Hz, 1H), 7.40 (dd, $J = 8.8$, 5.6 Hz, 1H), 7.21 (dd, $J = 9.6$, 3.0 Hz, 1H), 7.15 (td, $J = 8.6$, 3.1 Hz, 1H), 3.65 (s, 2H). ^{13}C NMR (101 MHz, $\text{DMSO}-d_6$, δ) 172.0, 164.1, 159.8 (d, $J = 242.3$ Hz), 136.6, 134.3, 133.9 (d, $J = 8.6$ Hz), 132.7 (d, $J = 2.7$ Hz), 130.7, 130.3, 128.5 (d, $J = 8.6$ Hz), 126.8, 121.7, 117.5 (d, $J = 22.8$ Hz), 113.8 (d, $J = 21.8$ Hz), 37.3. ^{19}F NMR (376 MHz, $\text{DMSO}-d_6$, δ) –116.8. LCMS (method a) m/z : 352.0 $[\text{M} + \text{H}]^+$, $t_{\text{R}} = 0.84$ min.

Methyl 2-(2-(3-Bromobenzamido)-5-fluorophenyl)acetate (25). HCl (**4** M) in dioxane (**9.5** mL, **38** mmol) was added at 23 °C to a solution of 2-(2-(3-bromobenzamido)-5-fluorophenyl)acetic acid (**23**, **3.4** g, **9.54** mmol) in MeOH (**100** mL). The formed suspension was stirred at 23 °C for 16 h. The reaction mixture was concentrated and the crude product was purified by column chromatography (100% CH_2Cl_2) to provide the title product as a yellowish solid in **3.0** g (**86%**) yield. ^1H NMR (400 MHz, $\text{DMSO}-d_6$, δ) 10.09 (s, 1H), 8.08 (t, $J = 1.8$ Hz, 1H), 7.91 (dt, $J = 7.9$, 1.3 Hz, 1H), 7.80 (ddd, $J = 8.0$, 2.1, 1.0 Hz, 1H), 7.50 (t, $J = 7.9$ Hz, 1H), 7.37 (dd, $J = 8.7$, 5.5 Hz, 1H), 7.24 (dd, $J = 9.6$, 3.0 Hz, 1H), 7.17 (td, $J = 8.5$, 3.0 Hz, 1H), 3.74 (s, 2H), 3.52 (s, 3H). ^{13}C NMR (101 MHz, $\text{DMSO}-d_6$, δ) 170.8, 164.2, 159.9 (d, $J = 242.5$ Hz), 136.4, 134.3, 133.6 (d, $J = 8.6$ Hz), 132.6 (d, $J = 2.9$ Hz), 130.7, 130.3, 128.9 (d, $J = 8.7$ Hz), 126.7, 121.6, 117.5 (d, $J = 22.9$ Hz), 114.2 (d, $J = 22.1$ Hz), 51.7, 36.8. ^{19}F NMR (376 MHz, $\text{DMSO}-d_6$, δ) –116.4. LCMS (method a) m/z : 366.0 $[\text{M} + \text{H}]^+$, $t_{\text{R}} = 0.99$ min.

2-(2-(3-Bromo-2-fluorobenzamido)-5-fluorophenyl)acetic Acid (24). 5-Fluoroindolin-2-one (**5.0** g, **33.1** mmol) was dissolved in a 10% solution of NaOH (aq.) (**45.3** mL, **125** mmol) and the mixture was stirred at 100 °C for 16 h. After being cooled to 23 °C, concentrated HCl (**8.5** mL) was added and a half of the volume of this mixture was treated at 23 °C with the solution of 3-bromo-2-fluorobenzoyl chloride (**3.16** g, **13.3** mmol) in THF (**10** mL) and the reaction mixture was stirred at 23 °C for 16 h. The solid was filtered off, washed with water, and dried in high vacuum to provide the title product as a brown solid in **4.7** g (**92%**) yield. ^1H NMR (400 MHz, $\text{DMSO}-d_6$, δ) 12.43 (s, 1H), 10.04 (s, 1H), 7.88 (t, $J = 7.3$ Hz, 1H), 7.67 (t, $J = 7.0$ Hz, 1H), 7.51–7.42 (m, 1H), 7.29 (t, $J = 7.7$ Hz, 1H), 7.25–7.10 (m, 2H), 3.68 (s, 2H). ^{13}C NMR (101 MHz, $\text{DMSO}-d_6$, δ) 171.8, 162.0, 159.7 (d, $J = 242.4$ Hz), 155.2 (d, $J = 250.0$ Hz), 135.5, 133.1 (d, $J = 8.5$ Hz), 132.2 (d, $J = 2.8$ Hz), 129.5 (d, $J = 2.4$ Hz), 128.1 (d, $J = 8.4$ Hz), 126.0 (d, $J = 4.3$ Hz), 125.8 (d, $J = 3.1$ Hz), 117.5 (d, $J = 22.9$ Hz), 113.9 (d, $J = 22.0$ Hz), 109.0, 36.9. ^{19}F NMR (376 MHz, $\text{DMSO}-d_6$, δ) –108.7, –116.7. LCMS (method a) m/z : 372.1 $[\text{M} + \text{H}]^+$, $t_{\text{R}} = 0.82$ min.

Methyl 2-(2-(3-Bromo-2-fluorobenzamido)-5-fluorophenyl)acetate (26). HCl (4 M) in dioxane (11.7 mL, 46.7 mmol) was added at 23 °C to a solution of 2-(2-(3-bromo-2-fluorobenzamido)-5-fluorophenyl)acetic acid (**24**, 4.5 g, 11.7 mmol) in MeOH (100 mL), and the formed suspension was stirred at 23 °C for 16 h. After concentration, the crude product was purified by column chromatography (100% CH₂Cl₂) to provide the title product as a pale yellow solid in 4.4 g (98%) yield. ¹H NMR (400 MHz, DMSO-*d*₆, δ) 10.06 (s, 1H), 7.88 (ddd, *J* = 8.2, 6.7, 1.8 Hz, 1H), 7.65 (ddd, *J* = 7.8, 6.3, 1.7 Hz, 1H), 7.44 (dd, *J* = 8.8, 5.6 Hz, 1H), 7.30 (t, *J* = 7.9 Hz, 1H), 7.23 (dd, *J* = 9.6, 3.0 Hz, 1H), 7.18 (td, *J* = 8.5, 3.0 Hz, 1H), 3.78 (s, 2H), 3.59 (s, 3H). ¹³C NMR (101 MHz, DMSO-*d*₆, δ) 170.7, 162.1, 159.8 (d, *J* = 242.6 Hz), 155.2 (d, *J* = 249.4 Hz), 135.5, 132.7 (d, *J* = 8.5 Hz), 132.2 (d, *J* = 2.5 Hz), 129.4 (d, *J* = 2.1 Hz), 128.3 (d, *J* = 8.7 Hz), 126.0 (d, *J* = 4.3 Hz), 125.8 (d, *J* = 16.5 Hz), 117.6 (d, *J* = 22.9 Hz), 114.2 (d, *J* = 22.2 Hz), 108.9 (d, *J* = 21.4 Hz), 51.7, 36.5. ¹⁹F NMR (376 MHz, DMSO-*d*₆, δ) -108.9, -116.4. LCMS (method a) *m/z*: 384.1 [M + H]⁺, *t*_R = 0.99 min.

Methyl 2-(2-(3-(4,4,5,5-tetramethyl-1,3,2-dioxaborolan-2-yl)benzamido)phenyl)acetate (27). According to the general procedure for the preparation of boronesters, the reaction of methyl 2-(2-(3-bromobenzamido)phenyl)acetate (**21**, 7.5 g, 21.5 mmol) and bis(pinacolato)diboron (5.5 g, 21.5 mmol) provided the title product after column chromatography (0–30% ethyl acetate in cyclohexane) as a yellow sticky oil in 8.3 g (94%) yield. ¹H NMR (400 MHz, DMSO-*d*₆, δ) 10.07 (s, 1H), 8.22 (s, 1H), 8.06–7.99 (m, 1H), 7.86 (dt, *J* = 7.4, 1.2 Hz, 1H), 7.54 (t, *J* = 7.6 Hz, 1H), 7.38–7.29 (m, 3H), 7.24 (td, *J* = 7.3, 1.7 Hz, 1H), 3.73 (s, 2H), 3.53 (s, 3H), 1.33 (s, 12H). ¹³C NMR (101 MHz, DMSO-*d*₆, δ) 171.4, 165.5, 137.3, 136.7, 134.1, 133.6, 131.0, 130.9, 130.5, 128.0, 127.4, 126.9, 126.1, 83.9, 51.5, 37.2, 24.7 (the signal for boron α carbon not resolved). LCMS (method a) *m/z*: 396.2 [M + H]⁺, *t*_R = 1.11 min.

Methyl 2-(2-(2-Fluoro-3-(4,4,5,5-tetramethyl-1,3,2-dioxaborolan-2-yl)benzamido)phenyl)acetate (28). According to the general procedure for the preparation of boronesters, the reaction of methyl 2-(2-(3-bromo-2-fluorobenzamido)phenyl)acetate (**22**, 1.0 g, 2.7 mmol) and bis(pinacolato)diboron (0.77 g, 3 mmol) provided the title product after column chromatography (0–30% ethyl acetate in cyclohexane) as a yellow sticky oil in 0.80 g (62%) yield. ¹H NMR (400 MHz, DMSO-*d*₆, δ) 9.90 (s, 1H), 7.84–7.74 (m, 2H), 7.45 (d, *J* = 7.7 Hz, 1H), 7.38–7.27 (m, 3H), 7.26–7.20 (m, 1H), 3.77 (s, 2H), 3.61 (s, 3H), 1.33 (s, 12H). ¹³C NMR (101 MHz, DMSO-*d*₆, δ) 171.2, 163.0 (d, *J* = 254.5 Hz), 162.8, 138.7 (d, *J* = 8.4 Hz), 136.2, 133.6 (d, *J* = 3.6 Hz), 131.0, 130.0, 127.4, 126.3, 126.0, 124.4 (d, *J* = 17.2 Hz), 124.2 (d, *J* = 3.7 Hz), 83.9, 51.5, 36.8, 24.6 (the signal for boron α carbon not resolved). ¹⁹F NMR (376 MHz, DMSO-*d*₆, δ) -103.8. LCMS (method a) *m/z*: 414.4 [M + H]⁺, *t*_R = 1.09 min.

Methyl 2-(5-Fluoro-2-(3-(4,4,5,5-tetramethyl-1,3,2-dioxaborolan-2-yl)benzamido)phenyl)acetate (29). According to the general procedure for the preparation of boron esters, the reaction of methyl 2-(2-(3-bromobenzamido)-5-fluorophenyl)acetate (**25**, 700 mg, 1.9 mmol) and bis(pinacolato)diboron (534 mg, 2.1 mmol) provided the title product after column chromatography (0–60% ethyl acetate in cyclohexane) as a beige solid in 612 mg (77%) yield. ¹H NMR (400 MHz, DMSO-*d*₆, δ) 10.07 (s, 1H), 8.22 (s, 1H), 8.02 (d, *J* = 7.9 Hz, 1H), 7.87 (d, *J* = 7.3 Hz, 1H), 7.54 (t, *J* = 7.6 Hz, 1H), 7.36 (dd, *J* = 8.8, 5.6 Hz, 1H), 7.23 (dd, *J* = 9.6, 3.0 Hz, 1H), 7.16 (td, *J* = 8.5, 3.0 Hz, 1H), 3.74 (s, 2H), 3.54 (s, 3H), 1.33 (s, 12H). ¹³C NMR (101 MHz, DMSO-*d*₆, δ) 170.9, 165.7, 159.9 (d, *J* = 242.2 Hz), 137.4, 133.9, 133.6, 133.5, 133.0 (d, *J* = 2.6 Hz), 130.6, 128.9, 128.8, 128.0, 117.5 (d, *J* = 22.9 Hz), 114.1 (d, *J* = 22.1 Hz), 83.9, 51.6, 36.9, 24.7. ¹⁹F NMR (376 MHz, DMSO-*d*₆, δ) -116.8. LCMS (method a) *m/z*: 414.2 [M + H]⁺, *t*_R = 1.15 min.

Methyl 2-(5-Fluoro-2-(2-fluoro-3-(4,4,5,5-tetramethyl-1,3,2-dioxaborolan-2-yl)benzamido)phenyl)acetate (30). According to the general procedure for the preparation of boron esters, the reaction of methyl 2-(2-(3-bromo-2-fluorobenzamido)-5-fluorophenyl)acetate (**26**, 1.76 g, 4.6 mmol) and bis(pinacolato)diboron (1.28 g, 5.0 mmol) provided the title product after column chromatography (0–40% ethyl acetate in cyclohexane) as a beige solid in 2.1 g (86%)

yield. ¹H NMR (400 MHz, DMSO-*d*₆, δ) 9.91 (s, 1H), 7.83–7.74 (m, 2H), 7.43 (dd, *J* = 8.8, 5.6 Hz, 1H), 7.34 (t, *J* = 7.4 Hz, 1H), 7.22 (dd, *J* = 9.6, 3.0 Hz, 1H), 7.16 (td, *J* = 8.5, 3.1 Hz, 1H), 3.77 (s, 2H), 3.61 (s, 3H), 1.32 (s, 12H). ¹³C NMR (101 MHz, DMSO-*d*₆, δ) 170.7, 163.0, 162.9 (d, *J* = 254.6 Hz), 159.8 (d, *J* = 242.3 Hz), 138.7 (d, *J* = 8.4 Hz), 133.6 (d, *J* = 3.7 Hz), 132.7 (d, *J* = 8.5 Hz), 132.5 (d, *J* = 2.9 Hz), 128.3 (d, *J* = 8.7 Hz), 124.30, 124.19 (d, *J* = 3.7 Hz), 124.12, 117.5 (d, *J* = 22.9 Hz), 114.1 (d, *J* = 22.1 Hz), 83.9, 51.6, 36.5, 24.6. ¹⁹F NMR (376 MHz, DMSO-*d*₆, δ) -103.8, -116.7. LCMS (method a) *m/z*: 432.2 [M + H]⁺, *t*_R = 1.16 min.

tert-Butyl 5-Bromo-2-chlorobenzylcarbamate (31). DIPEA (1.25 mL, 7.14 mmol) and Boc₂O (1.26 mL, 5.40 mmol) were added at 23 °C to a solution of 5-bromo-2-chlorobenzyl amine (750 mg, 3.40 mmol) in CH₂Cl₂ (34 mL). After being stirred at 23 °C for 16 h, the mixture was treated with saturated NaHCO₃ (aq.) and extracted with CH₂Cl₂. The organic layers were washed with water and brine, dried (Na₂SO₄), and concentrated. The crude product was purified by column chromatography (0–20% ethyl acetate in cyclohexane) to provide the title product as a pale yellow solid in 905 mg (83%) yield. ¹H NMR (400 MHz, DMSO-*d*₆, δ) 7.50–7.44 (m, 2H), 7.44–7.42 (m, 1H), 7.40 (d, *J* = 8.5 Hz, 1H), 4.18 (d, *J* = 6.2 Hz, 2H), 1.41 (s, 9H). ¹³C NMR (101 MHz, DMSO-*d*₆, δ) 155.7, 139.5, 131.2, 131.1, 131.0, 130.8, 120.0, 78.3, 41.0, 28.1. LCMS (method a) *m/z*: 220.1 [M + H-Boc]⁺, *t*_R = 1.29 min.

tert-Butyl 2-(5-Bromo-2-chlorophenoxy)ethylcarbamate (32). A mixture of 5-bromo-2-chlorophenol (0.50 g, 2.34 mmol), *tert*-butyl (2-bromoethyl)carbamate (1.35 g, 5.84 mmol), and Cs₂CO₃ (1.92 g, 5.84 mmol) in DMF (4.7 mL) was stirred at 120 °C for 6 h. After being cooled to 23 °C, the reaction mixture was diluted with ether and washed with water. The organic phases were washed with 2 M NaOH, water, and brine; dried (Na₂SO₄); and concentrated. The crude product was purified by column chromatography (0–77% ethyl acetate in *n*-heptane) to provide the title product as a colorless oil in 768 mg (91%) yield. ¹H NMR (400 MHz, DMSO-*d*₆, δ) 7.40–7.33 (m, 2H), 7.15 (dd, *J* = 8.4, 2.2 Hz, 1H), 6.94 (t, *J* = 5.8 Hz, 1H), 4.08 (t, *J* = 5.8 Hz, 2H), 3.34–3.30 (m, 2H), 1.38 (s, 9H). LCMS (method a) *m/z*: 249.9 [M + H-Boc]⁺, *t*_R = 1.36 min.

tert-Butyl 3-(5-Bromo-2-chlorophenoxy)azetidine-1-carboxylate (33). According to the general procedure for phenol alkylation by mesylates, the reaction of 5-bromo-2-chlorophenol (300 mg, 1.45 mmol) and 1-(*tert*-butoxycarbonyl)-3-(methanesulfonyloxy)azetidine (363 mg, 1.45 mmol) provided the title product after column chromatography (0–20% ethyl acetate in cyclohexane) as a colorless solid in 259 mg (45%) yield. ¹H NMR (400 MHz, DMSO-*d*₆, δ) 7.43 (d, *J* = 8.4 Hz, 1H), 7.21 (dd, *J* = 8.4, 2.2 Hz, 1H), 7.09 (d, *J* = 2.2 Hz, 1H), 5.19–5.04 (m, 1H), 4.33 (dd, *J* = 9.2, 7.2 Hz, 2H), 3.81 (dd, *J* = 9.7, 3.6 Hz, 2H), 1.39 (s, 9H). ¹³C NMR (101 MHz, DMSO-*d*₆, δ) 155.5, 152.6, 131.7, 125.2, 121.0, 120.6, 116.8, 79.0, 67.0, 55.3, 28.0. LCMS (method a) *m/z*: 262.1 [M + H-Boc]⁺, *t*_R = 1.44 min.

tert-Butyl 3-(5-Bromo-2-chlorophenoxy)pyrrolidine-1-carboxylate (34). According to the general procedure for phenol alkylation by mesylates, the reaction of 5-bromo-2-chlorophenol (100 mg, 0.48 mmol) and *tert*-butyl 3-((methylsulfonyl)oxy)pyrrolidine-1-carboxylate (128 mg, 0.48 mmol) provided the title product after column chromatography (0–10% ethyl acetate in cyclohexane) as a colorless resin in 136 mg (72%) yield. ¹H NMR (400 MHz, DMSO-*d*₆, δ) 7.45 (d, *J* = 2.2 Hz, 1H), 7.40 (d, *J* = 8.4 Hz, 1H), 7.19 (dd, *J* = 8.5, 2.2 Hz, 1H), 5.29–5.06 (m, 1H), 3.60–3.47 (m, 1H), 3.46–3.31 (m, 3H), 2.21–1.96 (m, 2H), 1.40 + 1.39 (s, 9H). ¹³C NMR (101 MHz, DMSO-*d*₆, δ) 153.7, 153.1, 131.5, 124.9, 122.1, 120.4, 118.6, 78.5, (78.3 + 77.4), (51.2 + 51.0), (43.9 + 43.7), (30.8 + 30.0), 28.1. LCMS (method a) *m/z*: 276.1 [M + H-Boc]⁺, *t*_R = 1.44 min.

tert-Butyl 4-(5-Bromo-2-chlorophenoxy)piperidine-1-carboxylate (35). According to the general procedure for phenol alkylation by mesylates, the reaction of 5-bromo-2-chlorophenol (300 mg, 1.45 mmol) and *tert*-butyl 4-((methylsulfonyl)oxy)piperidine-1-carboxylate (404 mg, 1.45 mmol) provided the title product after column chromatography (0–10% ethyl acetate in cyclohexane) as a colorless resin in 321 mg (57%) yield. ¹H NMR (400 MHz, DMSO-*d*₆, δ) 7.48 (d, *J* = 2.2 Hz, 1H), 7.39 (d, *J* = 8.5 Hz, 1H), 7.16 (dd, *J* = 8.5, 2.2 Hz,

1H), 4.83–4.69 (m, 1H), 3.69–3.49 (m, 2H), 3.30–3.22 (m, 2H), 1.92–1.80 (m, 2H), 1.63–1.51 (m, 2H), 1.41 (s, 9H). ¹³C NMR (101 MHz, DMSO-*d*₆, δ) 153.9, 153.2, 131.5, 124.7, 122.1, 120.5, 118.8, 78.8, 73.5, 40.2, 30.0, 28.0. LCMS (method a) *m/z*: 290.0 [M + H-Boc]⁺, *t*_R = 1.56 min.

tert-Butyl 3-(5-Bromo-2-chlorophenoxy)piperidine-1-carboxylate (rac-36). According to the general procedure for phenol alkylation by mesylates, the reaction of 5-bromo-2-chlorophenol (300 mg, 1.45 mmol) and *tert*-butyl 3-((methylsulfonyl)oxy)piperidine-1-carboxylate (404 mg, 1.45 mmol) provided the title product after column chromatography (0–20% ethyl acetate in cyclohexane) as a colorless solid in 91 mg (16%) yield. For analytical data, see 36.

(R)-tert-Butyl 3-(5-Bromo-2-chlorophenoxy)piperidine-1-carboxylate (36). According to the general procedure for phenol alkylation by the Mitsunobu reaction, the reaction of (*S*)-1-*N*-Boc-3-hydroxypiperidine (485 mg, 2.4 mmol) and 5-bromo-2-chlorophenol (500 mg, 2.4 mmol) provided the title product after column chromatography (0–60% ethyl acetate in cyclohexane) as a colorless oil in 458 mg (43%) yield. ¹H NMR (400 MHz, DMSO-*d*₆, δ) 7.43 (d, *J* = 2.1 Hz, 1H), 7.38 (d, *J* = 8.5 Hz, 1H), 7.15 (dd, *J* = 8.4, 2.2 Hz, 1H), 4.71–4.53 (m, 1H), 3.97–3.65 (m, 1H), 3.61–3.33 (m, 1H), 3.30–3.17 (m, 1H), 3.08–2.90 (m, 1H), 1.94–1.69 (m, 3H), 1.53–1.43 (m, 1H), 1.16 (s, 9H). ¹³C NMR (101 MHz, DMSO-*d*₆, δ) 153.7, 153.3, 131.4, 124.6, 124.2, 120.3, 117.8, 78.3, 70.9, 45.3, 42.6, 28.7, 27.6, 20.4. LCMS (method a) *m/z*: 290.1 [M + H-Boc]⁺, *t*_R = 1.48 min. [α]_D²³ + 39.4 (c 1.0, MeOH).

(R)-tert-Butyl 3-(5-Bromo-2-chloro-4-fluorophenoxy)piperidine-1-carboxylate (37). According to the general procedure for phenol alkylation by the Mitsunobu reaction, the reaction of (*S*)-1-*N*-Boc-3-hydroxypiperidine (1.8 g, 8.9 mmol) and 5-bromo-2-chloro-4-fluorophenol (2.0 g, 8.9 mmol) provided the title product as a colorless oil in 1.53 g (42%) yield. ¹H NMR (400 MHz, DMSO-*d*₆, δ) 7.73–7.50 (m, 2H), 4.69–4.45 (m, 1H), 3.96–3.39 (m, 2H), 3.27–3.15 (m, 1H), 3.11–2.88 (m, 1H), 1.97–1.63 (m, 3H), 1.52–1.42 (m, 1H), 1.16 (s, 9H). ¹³C NMR (101 MHz, DMSO-*d*₆, δ) 151.0 (d, *J* = 256 Hz), 149.7, 122.0, 120.1, 118.8 (d, *J* = 2.3 Hz), 118.0 (d, *J* = 26.8 Hz), 106.6 (d, *J* = 22.1 Hz), 78.3, 71.5, 45.3, 42.7, 28.7, 27.7, 20.4. ¹⁹F NMR (376 MHz, DMSO-*d*₆, δ) –116.8. LCMS (method a) *m/z*: 408.4 [M + H]⁺, *t*_R = 1.51 min. [α]_D²³ + 30.7 (c 1.0, MeOH).

(R)-tert-Butyl 3-(3-Bromo-6-chloro-2-fluorophenoxy)piperidine-1-carboxylate (38). According to the general procedure for phenol alkylation by the Mitsunobu reaction, the reaction of (*S*)-1-*N*-Boc-3-hydroxypiperidine (0.75 g, 3.7 mmol) and 3-bromo-6-chloro-2-fluorophenol (0.60 g, 2.7 mmol) provided the title product after column chromatography (0–5% ethyl acetate in cyclohexane) in 877 mg (77%) yield. ¹H NMR (400 MHz, DMSO-*d*₆, δ) 7.48 (dd, *J* = 8.8, 6.9 Hz, 1H), 7.33 (dd, *J* = 8.8, 1.9 Hz, 1H), 4.45–4.19 (m, 1H), 3.74–3.33 (m, 3H), 3.28–3.08 (m, 1H), 1.99–1.86 (m, 1H), 1.85–1.66 (m, 2H), 1.52–1.41 (m, 1H), 1.32 (s, 9H). ¹³C NMR (101 MHz, DMSO-*d*₆, δ) 153.8, 152.7 (d, *J* = 242 Hz), 142.1 (d, *J* = 15 Hz), 127.8 (d, *J* = 9.1 Hz), 127.6 (d, *J* = 18 Hz), 126.5 (d, *J* = 3.4 Hz), 107.9 (d, *J* = 20 Hz), 78.7, 77.4, 47.1, 42.5, 29.3, 27.9, 20.9. ¹⁹F NMR (376 MHz, DMSO-*d*₆, δ) –119.6. LCMS (method a) *m/z*: 408.1 [M + H]⁺, *t*_R = 1.53 min. [α]_D²³ + 10.8 (c 1.0, MeOH).

Methyl 2-(4'-Chloro-[1,1'-biphenyl]-3-carboxamido)benzoate (39). Oxalyl chloride (1.1 mL, 12 mmol) and DMF (1 drop) were added rapidly at 23 °C to 4'-chloro-[1,1'-biphenyl]-3-carboxylic acid (0.28 g, 1.2 mmol) in CH₂Cl₂ (12 mL) and the reaction mixture was stirred at 23 °C for 2 h. After concentration in high vacuum, the residue was dissolved in CH₂Cl₂ (12 mL) and treated at 23 °C with methyl 2-aminobenzoate (0.17 mL, 1.26 mmol) and Et₃N (0.42 mL, 3.0 mmol). After being stirred at 23 °C for 20 h, the reaction mixture was quenched with saturated NaHCO₃ (aq.) and extracted with CH₂Cl₂. The combined organic layers were washed with water and brine, dried (Na₂SO₄), and concentrated. The crude product was purified by column chromatography (0–60% EtOAc in *n*-heptane) to provide the title compound as a white solid in 0.41 g (86%) yield. ¹H NMR (400 MHz, DMSO-*d*₆, δ) 11.57 (s, 1H), 8.51 (dd, *J* = 8.4, 1.2 Hz, 1H), 8.24 (t, *J* = 1.8 Hz, 1H), 8.02 (dd, *J* = 8.0, 1.7 Hz, 1H),

7.99–7.94 (m, 2H), 7.84–7.79 (m, 2H), 7.76–7.67 (m, 2H), 7.62–7.57 (m, 2H), 7.28 (ddd, *J* = 8.1, 7.4, 1.2 Hz, 1H), 3.89 (s, 3H). LCMS (method a) *m/z*: 366.1 [M + H]⁺, *t*_R = 1.41 min.

2-(4'-Chloro-[1,1'-biphenyl]-3-carboxamido)benzoic Acid (4). LiOH·H₂O (85 mg, 2.0 mmol) was added at 23 °C to a mixture of methyl 2-(4'-chloro-[1,1'-biphenyl]-3-carboxamido)benzoate (39, 0.40 g, 1.0 mmol) in MeOH (8 mL) and water (2 mL). After being stirred at 50 °C for 3 h, the mixture was concentrated and the crude product was treated with concentrated HCl (11 mL). After being stirred at 60 °C for 2 h and cooled to 23 °C, the suspension was filtered off, washed with water, and dried in vacuum to provide the product 4 as a white solid in 161 mg (45%) yield. ¹H NMR (400 MHz, DMSO-*d*₆, δ) 13.83 (s, 1H), 12.24 (s, 1H), 8.71 (d, *J* = 7.9 Hz, 1H), 8.21 (s, 1H), 8.07 (dd, *J* = 7.9, 1.5 Hz, 1H), 8.00–7.89 (m, 2H), 7.78 (d, *J* = 8.6 Hz, 2H), 7.74–7.63 (m, 2H), 7.58 (d, *J* = 8.5 Hz, 2H), 7.23 (td, *J* = 7.6, 1.2 Hz, 1H). ¹³C NMR (101 MHz, DMSO-*d*₆, δ) 170.0, 164.5, 141.0, 139.5, 138.2, 135.4, 134.3, 133.0, 131.3, 130.4, 129.8, 129.1, 128.6, 126.5, 125.1, 123.1, 120.0, 116.9. LCMS (method a) *m/z*: 352.3 [M + H]⁺, *t*_R = 1.37 min. LCMS (method b) *m/z*: 352.2 [M + H]⁺, *t*_R = 6.55 min. HRMS *m/z*: [M + H]⁺ calcd for C₂₀H₁₅ClNO₃ 352.0735; found 352.0736.

2-(2-(4'-Chloro-2-fluoro-[1,1'-biphenyl]-3-carboxamido)phenyl)acetic Acid (6). According to the general procedure for Suzuki coupling, the reaction of methyl 2-(2-(3-bromo-2-fluorobenzamido)phenyl)acetate (22, 150 mg, 0.41 mmol) and 2-(4-chlorophenyl)-4,4,5,5-tetramethyl-1,3,2-dioxaborolane (117 mg, 0.49 mmol) provided the title compound after column chromatography (0–50% ethyl acetate in cyclohexane) as a white powder in 130 mg (79%) yield. ¹H NMR (400 MHz, DMSO-*d*₆, δ) 12.35 (s, 1H), 9.98 (d, *J* = 1.6 Hz, 1H), 7.75–7.56 (m, 6H), 7.52 (d, *J* = 7.9 Hz, 1H), 7.42 (t, *J* = 7.6 Hz, 1H), 7.31 (t, *J* = 7.4 Hz, 2H), 7.22 (td, *J* = 7.7, 1.5 Hz, 1H), 3.69 (s, 2H). ¹³C NMR (101 MHz, DMSO-*d*₆, δ) 172.4, 162.7, 155.9 (d, *J* = 251.2 Hz), 136.1, 133.3 (d, *J* = 41.2 Hz), 132.8 (d, *J* = 3.2 Hz), 131.0, 130.8 (d, *J* = 3.0 Hz), 129.9 (d, *J* = 47.3 Hz), 129.6, 128.7, 127.8 (d, *J* = 14.2 Hz), 127.2, 125.9, 125.9, 125.3 (d, *J* = 16.5 Hz), 124.8 (d, *J* = 4.1 Hz), 37.2. ¹⁹F NMR (376 MHz, DMSO-*d*₆, δ) –119.8. LCMS (method a) *m/z*: 383.8 [M + H]⁺, *t*_R = 1.12 min. LCMS (method b) *m/z*: 384.2 [M + H]⁺, *t*_R = 5.41 min. HRMS *m/z*: [M + H]⁺ calcd for C₂₁H₁₆ClFNO₃ 384.0797; found 384.0797.

Methyl 2-(2-(3'-((*tert*-Butoxycarbonyl)amino)methyl)-4'-chloro-[1,1'-biphenyl]-3-carboxamido)phenyl)acetate (40). A mixture of methyl 2-(2-(3-(4,4,5,5-tetramethyl-1,3,2-dioxaborolan-2-yl)-benzamido)phenyl)acetate (27, 0.28 g, 0.67 mmol), *tert*-butyl 5-bromo-2-chlorobenzylcarbamate (31, 0.24 g, 0.67 mmol) and 2 M Na₂CO₃ (aq.) (1.0 mL, 2.0 mmol) in DMF (6.7 mL) was degassed with argon. PdCl₂dppf·CH₂Cl₂ (27 mg, 0.034 mmol) was added, and the reaction mixture was heated in a microwave oven at 80 °C for 30 min. After being cooled to 23 °C, the mixture was filtered over Celite and washed with ethyl acetate and the filtrate was concentrated. The crude product was purified by column chromatography (0–80% ethyl acetate in *n*-heptane) to provide the title product as a pale yellow resin in 0.30 g (87%) yield. ¹H NMR (400 MHz, DMSO-*d*₆, δ) 10.09 (s, 1H), 8.18 (t, *J* = 1.9 Hz, 1H), 7.93 (dt, *J* = 7.8, 1.4 Hz, 1H), 7.84 (d, *J* = 7.8 Hz, 1H), 7.72–7.66 (m, 2H), 7.64 (d, *J* = 7.8 Hz, 1H), 7.57 (d, *J* = 8.7 Hz, 1H), 7.50 (t, *J* = 5.6 Hz, 1H), 7.43–7.39 (m, 1H), 7.38–7.30 (m, 2H), 7.25 (td, *J* = 7.4, 1.5 Hz, 1H), 4.28 (d, *J* = 6.1 Hz, 2H), 3.76 (s, 2H), 3.51 (s, 3H), 1.40 (s, 9H). ¹³C NMR (101 MHz, DMSO-*d*₆, δ) 171.4, 165.3, 156.0, 139.2, 138.3, 137.4, 136.5, 135.3, 133.4, 132.9, 131.0, 130.9, 129.7, 129.5, 129.2, 127.5, 126.92, 126.84, 126.80, 126.2, 125.8, 78.2, 51.6, 41.4, 37.2, 28.2. LCMS (method a) *m/z*: 507.2 [M – H][–], *t*_R = 1.26 min.

2-(2-(3'-(Aminomethyl)-4'-chloro-[1,1'-biphenyl]-3-carboxamido)phenyl)acetic Acid (10). LiOH·H₂O (48 mg, 1.1 mmol) was added rapidly at 23 °C to a mixture of methyl 2-(2-(3'-((*tert*-butoxycarbonyl)amino)methyl)-4'-chloro-[1,1'-biphenyl]-3-carboxamido)phenyl)acetate (40, 0.29 g, 0.56 mmol) in MeOH (5 mL) and water (1.25 mL) and the mixture was stirred at 50 °C for 18 h. After being cooled to 23 °C, the mixture was concentrated and the residue was treated with CH₂Cl₂ (5 mL) followed by TFA (0.88 mL, 11.3 mmol). The mixture was stirred at 23 °C for 4 h. After

concentration, the crude product was purified by HPLC (Gilson SunFire 30 mm × 100 mm, 23 °C, eluent A: water + 0.1% TFA, B: acetonitrile + 0.1% TFA, gradient: 5–80% B in 10 min, 80–100% B in 0.5 min. Flow: 40 mL/min) to provide the title product (TFA salt) as a white powder in 165 mg (57%) yield. ¹H NMR (400 MHz, DMSO-*d*₆, δ) 12.38 (s, 1H), 10.14 (s, 1H), 8.41 (s, 3H), 8.29 (s, 1H), 8.04–7.97 (m, 2H), 7.93 (d, *J* = 7.8 Hz, 1H), 7.85 (dd, *J* = 8.4, 2.3 Hz, 1H), 7.73–7.63 (m, 2H), 7.47 (d, *J* = 7.6 Hz, 1H), 7.36 (d, *J* = 7.4 Hz, 1H), 7.32 (d, *J* = 7.7 Hz, 1H), 7.24 (t, *J* = 7.3 Hz, 1H), 4.26 (s, 2H), 3.69 (s, 2H). ¹³C NMR (101 MHz, DMSO-*d*₆, δ) 172.7, 165.1, 138.6, 136.6, 135.5, 132.5, 132.2, 131.0, 130.9, 130.1, 129.6, 129.2, 129.0, 128.5, 127.3, 127.2, 126.3, 126.0, 37.6 (three carbons missing). LCMS (method a) *m/z*: 395.2 [M + H]⁺, *t*_R = 0.56 min. LCMS (method b) *m/z*: 395.3 [M + H]⁺, *t*_R = 2.59 min. HRMS *m/z*: [M + H]⁺ calcd for C₂₂H₂₀ClN₂O₃, 395.1157; found 395.1156.

2-(2-(3'-(2-(tert-Butoxycarbonyl)amino)ethoxy)-4'-chloro-[1,1'-biphenyl]-3-carboxamido)phenyl)acetic Acid (41). A mixture of *tert*-butyl 2-(5-bromo-2-chlorophenoxy)ethylcarbamate (**32**, 747 mg, 2.1 mmol), methyl 2-(2-(3-(4,4,5,5-tetramethyl-1,3,2-dioxaborolan-2-yl)benzamido)phenyl)acetate (**27**, 0.86 g, 2.1 mmol), and Na₂CO₃ (3.10 mL, 6.20 mmol) in DMF (21 mL) was degassed with argon. After the addition of PdCl₂(dppf)·CH₂Cl₂ (84 mg, 0.10 mmol), the mixture was stirred at 80 °C for 1 h. The mixture was cooled to 23 °C, filtered over Celite, and washed with EtOAc. The filtrate was concentrated and the crude product was purified by column chromatography (0–75% ethyl acetate in *n*-heptane) to provide the intermediate methyl 2-(2-(3'-(2-(tert-butoxycarbonyl)amino)ethoxy)-4'-chloro-[1,1'-biphenyl]-3-carboxamido)phenyl)acetate as a yellow foam in 0.78 g (63%) yield. ¹H NMR (400 MHz, DMSO-*d*₆, δ) 10.08 (s, 1H), 8.21 (s, 1H), 8.00–7.86 (m, 2H), 7.62 (t, *J* = 7.7 Hz, 1H), 7.55 (d, *J* = 8.3 Hz, 1H), 7.50 (s, 1H), 7.44 (d, *J* = 6.5 Hz, 1H), 7.39–7.31 (m, 3H), 7.25 (td, *J* = 7.4, 1.5 Hz, 1H), 6.99 (t, *J* = 5.8 Hz, 1H), 4.20 (t, *J* = 6.0 Hz, 2H), 3.78 (s, 2H), 3.50 (s, 3H), 3.37 (dt, *J* = 6.2 Hz, 2H), 1.37 (s, 9H). ¹³C NMR (101 MHz, DMSO-*d*₆, δ) 171.5, 165.3, 155.7, 154.2, 139.8, 139.2, 136.5, 135.1, 131.0, 130.8, 130.4, 129.9, 129.1, 127.5, 127.2, 126.8, 126.2, 125.9, 121.3, 120.1, 112.5, 77.8, 67.7, 51.6, 37.3, 28.2, 24.9, 24.5. LCMS (method a) *m/z*: 537.3 [M – H][–], *t*_R = 1.33 min. LiOH·H₂O (35 mg, 0.84 mmol) was added at 23 °C to a mixture of products from the previous step (methyl 2-(2-(3'-(2-(tert-butoxycarbonyl)amino)ethoxy)-4'-chloro-[1,1'-biphenyl]-3-carboxamido)phenyl)acetate, 0.25 g, 0.42 mmol) in MeOH (3.3 mL) and water (0.84 mL), and the mixture was stirred at 23 °C for 4 h. The reaction mixture was then concentrated, and the residue was treated with 0.2 M HCl. The resulting suspension was filtered, and the solid was washed with water and dried in high vacuum to provide the title product as a white solid in 158 mg (70%). ¹H NMR (400 MHz, DMSO-*d*₆, δ) 12.35 (s, 1H), 10.17 (s, 1H), 8.24 (s, 1H), 7.95 (d, *J* = 1.7 Hz, 1H), 7.93 (d, *J* = 1.7 Hz, 1H), 7.62 (t, *J* = 7.7 Hz, 1H), 7.54 (d, *J* = 8.2 Hz, 1H), 7.53–7.47 (m, 2H), 7.40–7.29 (m, 3H), 7.22 (td, *J* = 7.4, 1.4 Hz, 1H), 7.00 (t, *J* = 5.6 Hz, 1H), 4.20 (t, *J* = 6.0 Hz, 2H), 3.69 (s, 2H), 3.37 (td, *J* = 6.2, 5.6 Hz, 2H), 1.37 (s, 9H). ¹³C NMR (101 MHz, DMSO-*d*₆, δ) 174.0, 164.2, 155.8, 154.3, 139.5, 138.8, 138.1, 135.9, 130.45, 130.30, 130.23, 129.27, 129.13, 127.4, 125.9, 125.6, 123.6, 122.6, 121.0, 119.3, 112.4, 77.3, 67.51, 67.45, 44.9, 28.2. LCMS (method a) *m/z*: 525.2 [M + H]⁺, *t*_R = 1.25 min.

2-(2-(3'-(2-Aminoethoxy)-4'-chloro-[1,1'-biphenyl]-3-carboxamido)phenyl)acetic Acid (11). TFA (0.85 mL, 10.9 mmol) was added at 23 °C to a solution of 2-(2-(3'-(2-(tert-butoxycarbonyl)amino)ethoxy)-4'-chloro-[1,1'-biphenyl]-3-carboxamido)phenyl)acetic acid (**41**, 148 mg, 0.27 mmol) in CH₂Cl₂ (2.7 mL). After being stirred at 23 °C for 3 h, the reaction mixture was concentrated and the crude product was purified by HPLC (Gilson SunFire 30 mm × 100 mm; 23 °C, eluent A: water + 0.1% TFA, B: acetonitrile + 0.1% TFA, gradient: 5–80% B in 10 min, 80–100% B in 0.5 min. Flow: 40 mL/min) to provide the title product (TFA-salt) as a white powder in 120 mg (81%) yield. ¹H NMR (400 MHz, DMSO-*d*₆, δ) 12.45 (s, 1H), 10.11 (s, 1H), 8.23 (s, 1H), 8.02 (s, 3H), 7.98–7.89 (m, 2H), 7.64 (t, *J* = 7.7 Hz, 1H), 7.60 (d, *J* = 8.3 Hz, 1H), 7.53 (d, *J* = 2.0 Hz, 1H), 7.49 (d, *J* = 7.8 Hz, 1H), 7.43 (dd,

J = 8.2, 2.0 Hz, 1H), 7.39–7.28 (m, 2H), 7.23 (td, *J* = 7.4, 1.4 Hz, 1H), 4.41 (t, *J* = 5.2 Hz, 2H), 3.70 (s, 2H), 3.36–3.27 (m, 2H). ¹³C NMR (101 MHz, DMSO-*d*₆, δ) 172.8, 165.1, 153.7, 140.0, 139.1, 136.6, 135.3, 131.1, 130.8, 130.6, 129.9, 129.2, 127.25, 127.18, 126.3, 125.99, 125.89, 121.6, 120.9, 113.1, 66.0, 48.6, 37.7. LCMS (method a) *m/z*: 425.1 [M + H]⁺, *t*_R = 0.68 min. LCMS (method b) *m/z*: 425.1 [M + H]⁺, *t*_R = 3.13 min. HRMS *m/z*: [M + H]⁺ calcd for C₂₃H₂₂ClN₂O₄, 425.1263; found 425.1263.

2-(2-(3'-((1-(tert-Butoxycarbonyl)azetid-3-yl)oxy)-4'-chloro-[1,1'-biphenyl]-3-carboxamido)phenyl)acetic Acid (42). According to the general procedure for Suzuki coupling, the reaction of *tert*-butyl 3-(5-bromo-2-chlorophenoxy)azetid-1-carboxylate (**33**, 80 mg, 0.22 mmol) and methyl 2-(2-(3-(4,4,5,5-tetramethyl-1,3,2-dioxaborolan-2-yl)benzamido)phenyl)acetate (**27**, 87 mg, 0.22 mmol) provided the title product after column chromatography (0–10% MeOH in CH₂Cl₂) as a colorless solid in 114 mg (92%) yield. ¹H NMR (400 MHz, DMSO-*d*₆, δ) 12.37 (s, 1H), 10.11 (s, 1H), 8.22 (s, 1H), 8.01–7.85 (m, 2H), 7.68–7.56 (m, 2H), 7.53 (d, *J* = 7.9 Hz, 1H), 7.42 (d, *J* = 8.3 Hz, 1H), 7.38–7.28 (m, 2H), 7.23 (t, *J* = 7.5 Hz, 1H), 7.18 (s, 1H), 5.35–5.20 (m, 1H), 4.50–4.30 (m, 2H), 3.97–3.83 (m, 2H), 3.72 (s, 2H), 1.40 (s, 9H). ¹³C NMR (101 MHz, DMSO-*d*₆, δ) 172.8, 165.2, 155.5, 152.2, 140.1, 139.0, 136.6, 135.3, 131.1, 130.74, 130.68, 130.0, 129.2, 127.31, 127.25, 126.2, 126.0, 125.8, 121.3, 120.9, 112.3, 79.0, 66.8, 56.0, 37.8, 28.0. LCMS (method a) *m/z*: 535.3 [M – H][–], *t*_R = 1.33 min.

2-(2-(3'-(Azetid-3-yloxy)-4'-chloro-[1,1'-biphenyl]-3-carboxamido)phenyl)acetic Acid (12). Following the general procedure for Boc-cleavage with HCl, 2-(2-(3'-((1-(tert-butoxycarbonyl)azetid-3-yl)oxy)-4'-chloro-[1,1'-biphenyl]-3-carboxamido)phenyl)acetic acid (**42**, 100 mg, 0.19 mmol) provided the title product (HCl salt) as a colorless solid in 60 mg (92%) yield. ¹H NMR (400 MHz, DMSO-*d*₆, δ) 13.44 (s, 1H), 8.72 (s, 1H), 8.10 (d, *J* = 8.0 Hz, 1H), 8.01 (d, *J* = 1.6 Hz, 1H), 7.99 (d, *J* = 1.6 Hz, 1H), 7.78 (s, 1H), 7.64 (t, *J* = 7.7 Hz, 1H), 7.58 (d, *J* = 8.3 Hz, 1H), 7.54 (dd, *J* = 8.3, 1.6 Hz, 1H), 7.27–7.19 (m, 3H), 7.04 (td, *J* = 7.4, 1.3 Hz, 1H), 6.65 (s, 2H), 5.78 (p, *J* = 6.9 Hz, 1H), 4.44 (t, *J* = 8.1 Hz, 2H), 4.12 (t, *J* = 8.6 Hz, 2H), 3.56 (s, 2H). ¹³C NMR (101 MHz, DMSO-*d*₆, δ) 172.9, 165.3, 151.9, 140.3, 138.8, 136.7, 135.3, 131.1, 130.9, 130.8, 130.2, 129.2, 127.5, 127.3, 126.5, 126.3, 125.9, 121.4, 121.3, 112.9, 68.4, 52.0, 37.4. LCMS (method a) *m/z*: 437.2 [M + H]⁺, *t*_R = 0.72 min. LCMS (method b) *m/z*: 437.4 [M + H]⁺, *t*_R = 3.29 min. HRMS *m/z*: [M + H]⁺ calcd for C₂₄H₂₂ClN₂O₄, 437.1263; found 437.1263.

2-(2-(3'-((1-(tert-Butoxycarbonyl)pyrrolidin-3-yl)oxy)-4'-chloro-[1,1'-biphenyl]-3-carboxamido)phenyl)acetic Acid (43). According to the general procedure for Suzuki coupling, the reaction of *tert*-butyl 3-(5-bromo-2-chlorophenoxy)pyrrolidin-1-carboxylate (**34**, 90 mg, 0.23 mmol) and methyl 2-(2-(3-(4,4,5,5-tetramethyl-1,3,2-dioxaborolan-2-yl)benzamido)phenyl)acetate (**27**, 91 mg, 0.23 mmol) provided the title product after column chromatography (0–30% ethyl acetate in cyclohexane) as a colorless solid in 71 mg (56%) yield. ¹H NMR (400 MHz, DMSO-*d*₆, δ) 12.35 (s, 1H), 10.15 (s, 1H), 8.24 (s, 1H), 7.98–7.89 (m, 2H), 7.63 (t, *J* = 7.7 Hz, 1H), 7.59–7.49 (m, 3H), 7.40 (dd, *J* = 8.3, 2.1 Hz, 1H), 7.37–7.29 (m, 2H), 7.22 (td, *J* = 7.4, 1.5 Hz, 1H), 5.32 (s, 1H), 3.71 (s, 2H), 3.63–3.51 (m, 1H), 3.51–3.36 (m, 3H), 2.26–2.03 (m, 2H), 1.41 + 1.40 + 1.39 (s, 9H). ¹³C NMR (101 MHz, DMSO-*d*₆, δ) 172.8, 165.1, 153.7, 152.7, 139.9, 139.1, 136.6, 135.3, 131.0, 130.60, 130.60, 129.9, 129.1, 127.21, 126.2, 125.94, 125.78, 122.47, 122.40, 120.7, 114.4, 78.5, (78.1 + 77.2), (51.4 + 51.1), (44.0 + 43.7), 37.8, (31.0 + 30.1), 28.1. LCMS (method a) *m/z*: 551.1 [M + H]⁺, *t*_R = 1.31 min.

2-(2-(4'-Chloro-3'-(pyrrolidin-3-yloxy)-[1,1'-biphenyl]-3-carboxamido)phenyl)acetic Acid (13). Following the general procedure for Boc-cleavage with HCl, 2-(2-(3'-((1-(tert-butoxycarbonyl)pyrrolidin-3-yl)oxy)-4'-chloro-[1,1'-biphenyl]-3-carboxamido)phenyl)acetic acid (**43**, 60 mg, 0.11 mmol) provided the title product (HCl salt) as a colorless solid in 47 mg (85%) yield. ¹H NMR (400 MHz, DMSO-*d*₆, δ) 12.35 (s, 1H), 10.19 (s, 1H), 9.45 (s, 1H), 9.34 (s, 1H), 8.27 (s, 1H), 7.92–7.98 (m, 2H), 7.64 (t, *J* = 7.8 Hz, 1H), 7.61–7.57 (m, 2H), 7.52 (d, *J* = 7.7 Hz, 1H), 7.44 (dd, *J* =

8.3, 1.9 Hz, 1H), 7.37–7.29 (m, 2H), 7.23 (td, $J = 7.5$, 1.5 Hz, 1H), 5.46–5.39 (m, 1H), 3.72 (s, 2H), 3.64–3.58 (m, 1H), 3.48–3.34 (m, 3H), 2.29–2.19 (m, 2H). ^{13}C NMR (101 MHz, DMSO- d_6 , δ) 172.8, 165.1, 152.3, 140.0, 138.9, 136.6, 135.3, 131.01, 130.72, 130.67, 130.0, 129.1, 127.3, 127.2, 126.2, 126.0, 125.8, 122.3, 121.2, 114.5, 77.3, 49.8, 43.7, 37.8, 30.8. LCMS (method a) m/z : 451.1 $[\text{M} + \text{H}]^+$, $t_{\text{R}} = 0.72$ min. LCMS (method b) m/z : 451.1 $[\text{M} + \text{H}]^+$, $t_{\text{R}} = 3.26$ min. HRMS m/z : $[\text{M} + \text{H}]^+$ calcd for $\text{C}_{25}\text{H}_{24}\text{ClN}_2\text{O}_4$ 451.1419; found 451.1419.

2-(2-(3'-((1-(tert-Butoxycarbonyl)piperidin-4-yl)oxy)-4'-chloro-[1,1'-biphenyl]-3-carboxamido)phenyl)acetic Acid (44). According to the general procedure for Suzuki coupling, the reaction of methyl 2-(2-(3-(4,4,5,5-tetramethyl-1,3,2-dioxaborolan-2-yl)benzamido)phenyl)acetate (**27**, 81 mg, 0.21 mmol) and *tert*-butyl 4-(5-bromo-2-chlorophenoxy)piperidine-1-carboxylate (**35**, 80 mg, 0.21 mmol) provided the title product after column chromatography (0–50% ethyl acetate in cyclohexane) as a colorless solid in 80 mg (69%) yield. ^1H NMR (400 MHz, DMSO- d_6 , δ) 12.36 (s, 1H), 10.27 (s, 1H), 8.25 (s, 1H), 7.97–7.89 (m, 2H), 7.62 (t, $J = 7.8$ Hz, 1H), 7.59–7.51 (m, 3H), 7.37 (dd, $J = 8.3$, 2.1 Hz, 1H), 7.35–7.29 (m, 2H), 7.21 (td, $J = 7.4$, 1.4 Hz, 1H), 4.96–4.82 (m, 1H), 3.70 (s, 2H), 3.61 (ddd, $J = 10.8$, 8.9, 5.1 Hz, 2H), 3.29–3.25 (m, 2H), 2.01–1.85 (m, 2H), 1.72–1.58 (m, 2H), 1.41 (s, 9H). ^{13}C NMR (101 MHz, DMSO- d_6 , δ) 172.8, 165.1, 153.9, 152.7, 139.9, 139.1, 136.7, 135.3, 131.0, 130.62, 130.55, 129.9, 129.1, 127.22, 127.15, 126.03, 125.91, 125.67, 122.6, 120.5, 114.8, 78.7, 73.2, 69.2, 30.2, 28.1, 24.9. LCMS (method a) m/z : 565.2 $[\text{M} + \text{H}]^+$, $t_{\text{R}} = 1.38$ min.

2-(2-(4'-Chloro-3'-(piperidin-4-yloxy)-[1,1'-biphenyl]-3-carboxamido)phenyl)acetic Acid (14). Following the general procedure for Boc-cleavage with HCl, 2-(2-(3'-((1-(tert-butoxycarbonyl)piperidin-4-yl)oxy)-4'-chloro-[1,1'-biphenyl]-3-carboxamido)phenyl)acetic acid (**44**, 70 mg, 0.12 mmol) provided the title product (HCl-salt) as a colorless solid in 52 mg (84%) yield. ^1H NMR (400 MHz, DMSO- d_6 , δ) 12.36 (s, 1H), 10.18 (s, 1H), 8.80 (s, 2H), 8.25 (s, 1H), 7.95 (d, $J = 7.8$ Hz, 1H), 7.92 (d, $J = 8.3$ Hz, 1H), 7.67–7.61 (m, 2H), 7.58 (d, $J = 8.3$ Hz, 1H), 7.52 (d, $J = 6.7$ Hz, 1H), 7.40 (dd, $J = 8.3$, 2.1 Hz, 1H), 7.37–7.29 (m, 2H), 7.23 (td, $J = 7.5$, 1.5 Hz, 1H), 5.06–4.91 (m, 1H), 3.72 (s, 2H), 3.28–3.19 (m, 2H), 3.18–3.06 (m, 2H), 2.22–2.07 (m, 2H), 2.02–1.87 (m, 2H). ^{13}C NMR (101 MHz, DMSO- d_6 , δ) 172.8, 165.1, 152.3, 140.1, 139.1, 138.6, 136.6, 135.3, 131.0, 130.7, 130.0, 129.1, 127.3, 127.2, 126.3, 126.0, 125.8, 122.5, 120.9, 114.8, 70.6, 40.4, 37.7, 27.0. LCMS (method a) m/z : 465.3 $[\text{M} + \text{H}]^+$, $t_{\text{R}} = 0.65$ min. LCMS (method a) m/z : 465.3 $[\text{M} + \text{H}]^+$, $t_{\text{R}} = 0.65$ min. LCMS (method b) m/z : 465.3 $[\text{M} + \text{H}]^+$, $t_{\text{R}} = 3.17$ min. HRMS m/z : $[\text{M} - \text{H}]^-$ calcd for $\text{C}_{26}\text{H}_{24}\text{ClN}_2\text{O}_4$ 463.1430; found 463.1431.

2-(2-(3'-((1-(tert-Butoxycarbonyl)piperidin-3-yl)oxy)-4'-chloro-[1,1'-biphenyl]-3-carboxamido)phenyl)acetic Acid (45). According to the general procedure for Suzuki coupling, the reaction of methyl 2-(2-(3-(4,4,5,5-tetramethyl-1,3,2-dioxaborolan-2-yl)benzamido)phenyl)acetate (**27**, 86 mg, 0.22 mmol) and *tert*-butyl 3-(5-bromo-2-chlorophenoxy)piperidine-1-carboxylate (*rac*-**36**, 85 mg, 0.22 mmol) provided the title product after column chromatography (0–50% ethyl acetate in cyclohexane) as a colorless solid in 117 mg (90%) yield. ^1H NMR (400 MHz, DMSO- d_6 , δ) 12.42 (s, 1H), 10.22 (s, 1H), 8.23 (s, 1H), 7.94 (d, $J = 7.8$ Hz, 1H), 7.92–7.84 (m, 1H), 7.62 (t, $J = 7.7$ Hz, 1H), 7.57–7.47 (m, 3H), 7.39–7.28 (m, 3H), 7.22 (td, $J = 7.4$, 1.4 Hz, 1H), 4.77 (s, 1H), 4.00–3.87 (m, 1H), 3.69 (s, 2H), 3.61–3.40 (m, 3H), 1.85 (s, 3H), 1.54–1.45 (m, 1H), 1.40 (s, 9H). LCMS (method a) m/z : 563.4 $[\text{M} - \text{H}]^-$, $t_{\text{R}} = 1.32$ min.

2-(2-(4'-Chloro-3'-(piperidin-3-yloxy)-[1,1'-biphenyl]-3-carboxamido)phenyl)acetic Acid (15). Following the general procedure for Boc-cleavage with HCl, 2-(2-(3'-((1-(tert-butoxycarbonyl)piperidin-3-yl)oxy)-4'-chloro-[1,1'-biphenyl]-3-carboxamido)phenyl)acetic acid (**45**, 105 mg, 0.19 mmol) provided the title product (HCl salt) as a colorless solid in 50 mg (53%) yield. ^1H NMR (400 MHz, DMSO- d_6 , δ) 12.32 (s, 1H), 10.26 (s, 1H), 9.34 (s, 1H), 8.84 (s, 1H), 8.31 (s, 1H), 7.98–7.91 (m, 2H), 7.75 (d, $J = 2.2$ Hz, 1H), 7.63 (t, $J = 7.7$ Hz, 1H), 7.59 (d, $J = 8.2$ Hz, 1H), 7.51 (d, $J = 7.8$ Hz, 1H), 7.44 (dd, $J = 8.3$, 2.0 Hz, 1H), 7.34 (dd, $J = 7.3$,

1.7 Hz, 1H), 7.31 (dd, $J = 7.7$, 1.8 Hz, 1H), 7.22 (td, $J = 7.5$, 1.5 Hz, 1H), 5.03–4.92 (m, 1H), 3.72 (s, 2H), 3.44 (d, $J = 11.9$ Hz, 1H), 3.24–3.10 (m, 2H), 3.09–2.97 (m, 1H), 2.11–1.92 (m, 2H), 1.92–1.70 (m, 2H). ^{13}C NMR (101 MHz, DMSO- d_6 , δ) 172.8, 165.1, 152.6, 140.1, 138.9, 136.6, 135.2, 131.0, 130.79, 130.72, 130.0, 129.1, 127.4, 127.1, 126.4, 126.1, 125.8, 122.6, 121.3, 115.2, 70.9, 45.3, 42.7, 37.8, 27.2, 19.0. LCMS (method a) m/z : 465.2 $[\text{M} + \text{H}]^+$, $t_{\text{R}} = 0.86$ min. LCMS (method b) m/z : 465.0 $[\text{M} + \text{H}]^+$, $t_{\text{R}} = 4.02$ min. HRMS m/z : $[\text{M} + \text{H}]^+$ calcd for $\text{C}_{26}\text{H}_{26}\text{ClN}_2\text{O}_4$ 465.1576; found 465.1578.

(R)-2-(2-(3'-((1-(tert-Butoxycarbonyl)piperidin-3-yl)oxy)-4'-chloro-2-fluoro-[1,1'-biphenyl]-3-carboxamido)phenyl)acetic Acid (46). According to the general procedure for Suzuki coupling, the reaction of (*R*)-*tert*-butyl 3-(5-bromo-2-chlorophenoxy)piperidine-1-carboxylate (**36**, 95 mg, 0.24 mmol) and methyl 2-(2-(2-fluoro-3-(4,4,5,5-tetramethyl-1,3,2-dioxaborolan-2-yl)benzamido)phenyl)acetate (**28**, 100 mg, 0.24 mmol) provided the title product after column chromatography (0–60% ethyl acetate in cyclohexane) as a colorless solid in 129 mg (86%) yield. ^1H NMR (400 MHz, DMSO- d_6 , δ) 12.15 (s, 1H), 10.05 (s, 1H), 7.77–7.67 (m, 2H), 7.65 (d, $J = 9.1$ Hz, 1H), 7.58–7.51 (m, 2H), 7.42 (t, $J = 7.6$ Hz, 1H), 7.32 (d, $J = 7.6$ Hz, 1H), 7.28–7.13 (m, 3H), 4.77–4.52 (m, 1H), 3.81–3.71 (m, 1H), 3.68 (s, 2H), 3.46–3.38 (m, 3H), 1.95–1.77 (m, 3H), 1.51–1.45 (m, 1H), 1.12 (s, 9H). ^{13}C NMR (101 MHz, DMSO- d_6 , δ) 172.5, 162.7, 155.9 (d, $J = 251.5$ Hz), 153.7, 152.4, 151.7 (d, $J = 4.6$ Hz), 136.1, 134.7, 132.9, 131.0, 130.8 (d, $J = 7.4$ Hz), 130.2, 130.0, 129.6, 127.2, 125.8 (d, $J = 4.8$ Hz), 125.3 (d, $J = 16.3$ Hz), 124.7 (d, $J = 4.1$ Hz), 124.4, 122.0, 115.5 (d, $J = 4.3$ Hz), 78.2, 70.6, 45.4, 42.7, 37.4, 28.8, 27.6, 20.5. ^{19}F NMR (376 MHz, DMSO- d_6 , δ) –119.5. LCMS (method a) m/z : 581.3 $[\text{M} - \text{H}]^-$, $t_{\text{R}} = 1.30$ min. $[\alpha]_{\text{D}}^{23} + 26.2$ (c 1.0, MeOH).

(R)-2-(2-(4'-Chloro-2-fluoro-3'-(piperidin-3-yloxy)-[1,1'-biphenyl]-3-carboxamido)phenyl)acetic Acid (16). Following the general procedure for Boc-cleavage with HCl, (*R*)-2-(2-(3'-((1-(tert-butoxycarbonyl)piperidin-3-yl)oxy)-4'-chloro-2-fluoro-[1,1'-biphenyl]-3-carboxamido)phenyl)acetic acid (**46**, 120 mg, 0.2 mmol) provided the title product (HCl-salt) as a colorless solid in 70 mg (65%) yield. ^1H NMR (400 MHz, DMSO- d_6 , δ) 12.36 (s, 1H), 10.03 (s, 1H), 9.37 (s, 1H), 8.87 (s, 1H), 7.80–7.66 (m, 2H), 7.61 (d, $J = 8.2$ Hz, 1H), 7.57–7.47 (m, 2H), 7.43 (t, $J = 7.6$ Hz, 1H), 7.36–7.15 (m, 4H), 4.90–4.77 (m, 1H), 3.70 (s, 2H), 3.50–3.25 (m, 3H), 3.13–2.96 (m, 2H), 2.10–1.91 (m, 2H), 1.90–1.68 (m, 2H). ^{13}C NMR (101 MHz, DMSO- d_6 , δ) 172.5, 162.7, 155.9 (d, $J = 251.7$ Hz), 152.2, 136.1, 135.0, 133.0 (d, $J = 2.9$ Hz), 131.1, 130.5, 130.1, 129.8 (d, $J = 2.6$ Hz), 127.9 (d, $J = 13.8$ Hz), 127.2, 125.9, 125.3 (d, $J = 16.1$ Hz), 124.73, 124.70, 123.5 (d, $J = 2.2$ Hz), 123.0, 117.4 (d, $J = 2.6$ Hz), 71.0, 45.3, 42.6, 37.3, 27.0, 18.8. ^{19}F NMR (376 MHz, DMSO- d_6 , δ) –119.0. LCMS (method a) m/z : 483.2 $[\text{M} + \text{H}]^+$, $t_{\text{R}} = 0.72$ min. LCMS (method b) m/z : 483.2 $[\text{M} + \text{H}]^+$, $t_{\text{R}} = 3.28$ min. HRMS m/z : $[\text{M} + \text{H}]^+$ calcd for $\text{C}_{26}\text{H}_{25}\text{ClF}_2\text{N}_2\text{O}_4$ 483.1481; found 483.1482. $[\alpha]_{\text{D}}^{23} + 1.4$ (c 1.0, MeOH).

(R)-2-(2-(3'-((1-(tert-Butoxycarbonyl)piperidin-3-yl)oxy)-4'-chloro-2-fluoro-[1,1'-biphenyl]-3-carboxamido)phenyl)acetic Acid (47). According to the general procedure for Suzuki coupling, the reaction of (*R*)-*tert*-butyl 3-(3-bromo-6-chloro-2-fluorophenoxy)piperidine-1-carboxylate (**38**, 103 mg, 0.25 mmol) and methyl 2-(2-(3-(4,4,5,5-tetramethyl-1,3,2-dioxaborolan-2-yl)benzamido)phenyl)acetate (**27**, 100 mg, 0.25 mmol) provided the title product after column chromatography (0–5% MeOH in CH_2Cl_2) as a colorless resin in 108 mg (70%) yield. ^1H NMR (400 MHz, DMSO- d_6 , δ) 12.34 (s, 1H), 10.11 (s, 1H), 8.10 (s, 1H), 8.00 (d, $J = 7.7$ Hz, 1H), 7.78 (d, $J = 7.7$ Hz, 1H), 7.65 (t, $J = 7.7$ Hz, 1H), 7.50–7.43 (m, 2H), 7.42–7.28 (m, 3H), 7.23 (td, $J = 7.5$, 1.4 Hz, 1H), 4.44–4.18 (m, 1H), 3.85–3.68 (m, 1H), 3.67 (s, 2H), 3.64–3.52 (m, 1H), 3.49–3.35 (m, 1H), 3.29–3.10 (m, 1H), 2.12–1.70 (m, 3H), 1.52–1.41 (m, 1H), 1.30 (s, 9H). ^{13}C NMR (101 MHz, DMSO- d_6 , δ) 172.8, 164.9, 153.9, 153.0 (d, $J = 252.1$ Hz), 141.8 (d, $J = 14.5$ Hz), 136.6, 135.1, 134.2, 131.9 (d, $J = 3.4$ Hz), 131.0, 130.8, 128.8, 128.2 (d, $J = 12.2$ Hz), 127.9, 127.5, 127.2, 126.2, 125.78, 125.70 (d, $J = 3.8$ Hz), 125.30, 125.22, 78.7, (77.55 + 77.46), (47.4 + 46.6), (43.5 + 42.7), 38.0, 29.5, 27.9, (22.1 + 21.2). ^{19}F NMR (376 MHz, DMSO- d_6 , δ)

–131.2. LCMS (method a) m/z : 583.3 $[M + H]^+$, $t_R = 1.33$ min. $[\alpha]_D^{23} + 13.3$ (c 1.0, MeOH).

(*R*)-2-(2-(3'-((1-(*tert*-butoxycarbonyl)piperidin-3-yl)oxy)-4'-chloro-2'-fluoro-[1,1'-biphenyl]-3-carboxamido)phenyl)acetic Acid (**17**). Following the general procedure for Boc-cleavage with HCl, (*R*)-2-(2-(3'-((1-(*tert*-butoxycarbonyl)piperidin-3-yl)oxy)-4'-chloro-2'-fluoro-[1,1'-biphenyl]-3-carboxamido)phenyl)acetic acid (**47**, 97 mg, 0.17 mmol) provided the title product (HCl salt) as a colorless solid in 76 mg (88%) yield. $^1\text{H NMR}$ (400 MHz, DMSO- d_6 , δ) 12.33 (s, 1H), 10.12 (s, 1H), 9.10 (s, 1H), 8.84 (s, 1H), 8.12 (s, 1H), 8.02 (d, $J = 7.8$ Hz, 1H), 7.79 (d, $J = 7.0$ Hz, 1H), 7.66 (t, $J = 7.8$ Hz, 1H), 7.53 (d, $J = 9.5$ Hz, 1H), 7.49–7.42 (m, 2H), 7.37–7.28 (m, 2H), 7.23 (td, $J = 7.4$, 1.5 Hz, 1H), 4.48 (tt, $J = 7.0$, 3.3 Hz, 1H), 3.68 (s, 2H), 3.48–3.37 (m, 2H), 3.16–2.97 (m, 2H), 2.11–1.96 (m, 2H), 1.96–1.82 (m, 1H), 1.79–1.65 (m, 1H). $^{13}\text{C NMR}$ (101 MHz, DMSO- d_6 , δ) 172.7, 164.9, 153.1 (d, $J = 249.6$ Hz), 141.9 (d, $J = 13.4$ Hz), 136.5, 135.1, 134.0, 131.9, 131.0, 130.8, 128.9, 128.3, 128.0, 127.5 (d, $J = 9.0$ Hz), 127.4, 127.2, 126.4, 126.2 (d, $J = 2.7$ Hz), 125.93, 125.79 (d, $J = 3.1$ Hz), 76.3, 46.2, 42.8, 37.6, 27.4, 18.7. $^{19}\text{F NMR}$ (376 MHz, DMSO- d_6 , δ) –130.8. LCMS (method a) m/z : 483.2 $[M + H]^+$, $t_R = 0.73$ min. LCMS (method b) m/z : 483.1 $[M + H]^+$, $t_R = 3.18$ min. HRMS m/z : $[M + H]^+$ calcd for $\text{C}_{26}\text{H}_{25}\text{ClF}_2\text{N}_2\text{O}_4$ 483.1481; found 483.1484. $[\alpha]_D^{23} + 2.2$ (c 0.5, MeOH).

(*R*)-2-(2-(3'-((1-(*tert*-butoxycarbonyl)piperidin-3-yl)oxy)-4'-chloro-2'-fluoro-[1,1'-biphenyl]-3-carboxamido)-5-fluorophenyl)acetic Acid (**48**). According to the general procedure for Suzuki coupling, the reaction of (*R*)-*tert*-butyl 3-(3-bromo-6-chloro-2-fluorophenoxy)piperidine-1-carboxylate (**38**, 99 mg, 0.24 mmol) and methyl 2-(5-fluoro-2-(3-(4,4,5,5-tetramethyl-1,3,2-dioxaborolan-2-yl)benzamido)phenyl)acetate (**29**, 100 mg, 0.24 mmol) provided the title product after column chromatography (0–5% MeOH in CH_2Cl_2) as a colorless resin in 113 mg (70%) yield. $^1\text{H NMR}$ (400 MHz, DMSO- d_6 , δ) 12.39 (s, 1H), 10.16 (s, 1H), 8.09 (s, 1H), 7.99 (d, $J = 7.7$ Hz, 1H), 7.77 (d, $J = 7.7$ Hz, 1H), 7.64 (t, $J = 7.7$ Hz, 1H), 7.50–7.35 (m, 3H), 7.22 (dd, $J = 9.7$, 3.0 Hz, 1H), 7.16 (td, $J = 8.5$, 3.0 Hz, 1H), 4.47–4.17 (m, 1H), 3.67 (s, 2H), 3.63–3.49 (m, 1H), 3.43–3.19 (m, 3H), 2.07–1.66 (m, 3H), 1.47–1.41 (m, 1H), 1.33 (s, 9H). $^{13}\text{C NMR}$ (101 MHz, DMSO- d_6 , δ) 172.0, 165.1, 159.7 (d, $J = 242.0$ Hz), 153.9, 152.9 (d, $J = 251.3$ Hz), 141.8 (d, $J = 14.5$ Hz), 134.9, 134.2, 133.8 (d, $J = 8.5$ Hz), 132.9 (d, $J = 2.8$ Hz), 131.9, 128.8, 128.4 (d, $J = 8.7$ Hz), 128.2 (d, $J = 12.3$ Hz), 127.9 (d, $J = 2.2$ Hz), 127.50, 127.45, 125.7 (d, $J = 3.8$ Hz), 125.3, 117.4 (d, $J = 22.8$ Hz), 113.8 (d, $J = 22.1$ Hz), 78.7, (77.6 + 77.4), (47.4 + 46.6), (43.4 + 42.6), 37.3, 29.5, 27.9, (22.0 + 21.2). $^{19}\text{F NMR}$ (376 MHz, DMSO- d_6 , δ) –117.0, –131.2. LCMS (method a) m/z : 601.5 $[M + H]^+$, $t_R = 1.33$ min. $[\alpha]_D^{23} + 12.6$ (c 1.0, MeOH).

(*R*)-2-(2-(4'-Chloro-2'-fluoro-3'-(piperidin-3-yloxy)-[1,1'-biphenyl]-3-carboxamido)-5-fluorophenyl)acetic Acid (**18**). Following the general procedure for Boc-cleavage with HCl, (*R*)-2-(2-(3'-((1-(*tert*-butoxycarbonyl)piperidin-3-yl)oxy)-4'-chloro-2'-fluoro-[1,1'-biphenyl]-3-carboxamido)-5-fluorophenyl)acetic acid (**48**, 113 mg, 0.17 mmol) provided the title product (HCl salt) as a colorless solid in 73 mg (80%) yield. $^1\text{H NMR}$ (400 MHz, DMSO- d_6 , δ) 12.39 (s, 1H), 10.16 (s, 1H), 9.45 (s, 1H), 9.01 (s, 1H), 8.12 (s, 1H), 8.01 (d, $J = 7.8$ Hz, 1H), 7.79 (d, $J = 7.6$ Hz, 1H), 7.66 (t, $J = 7.8$ Hz, 1H), 7.52 (d, $J = 9.3$ Hz, 1H), 7.49–7.38 (m, 2H), 7.23 (dd, $J = 9.7$, 3.0 Hz, 1H), 7.16 (td, $J = 8.5$, 3.1 Hz, 1H), 4.57–4.39 (m, 1H), 3.69 (s, 2H), 3.50–3.30 (m, 1H), 3.23 (dd, $J = 12.4$, 7.2 Hz, 1H), 3.16–2.93 (m, 2H), 2.11–1.97 (m, 2H), 1.94–1.82 (m, 1H), 1.80–1.65 (m, 1H). $^{13}\text{C NMR}$ (101 MHz, DMSO- d_6 , δ) 172.0, 165.1, 159.8 (d, $J = 242.1$ Hz), 153.1 (d, $J = 249.8$ Hz), 141.8 (d, $J = 14.8$ Hz), 134.9, 133.9, 133.8 (d, $J = 8.5$ Hz), 132.8 (d, $J = 2.9$ Hz), 131.9 (d, $J = 3.2$ Hz), 128.8, 128.5 (d, $J = 8.6$ Hz), 128.3 (d, $J = 12.2$ Hz), 128.0, 127.6, 127.5 (d, $J = 2.4$ Hz), 126.2 (d, $J = 3.4$ Hz), 125.8 (d, $J = 4.1$ Hz), 117.4 (d, $J = 22.8$ Hz), 113.8 (d, $J = 22.1$ Hz), 76.3, 46.1, 42.7, 37.2, 27.6, 18.8. $^{19}\text{F NMR}$ (376 MHz, DMSO- d_6 , δ) –116.9, –130.7. LCMS (method a) m/z : 501.2 $[M + H]^+$, $t_R = 0.73$ min. LCMS (method b) m/z : 501.2 $[M + H]^+$, $t_R = 3.35$ min. HRMS m/z : $[M + H]^+$ calcd for $\text{C}_{26}\text{H}_{24}\text{ClF}_2\text{N}_2\text{O}_4$ 501.1387; found 501.1392. $[\alpha]_D^{23} + 1.5$ (c 1.0, MeOH).

(*R*)-2-(2-(5'-((1-(*tert*-butoxycarbonyl)piperidin-3-yl)oxy)-4'-chloro-2'-fluoro-[1,1'-biphenyl]-3-carboxamido)-5-fluorophenyl)acetic Acid (**49**). According to the general procedure for Suzuki coupling, the reaction of (*R*)-*tert*-butyl 3-(5-bromo-2-chloro-4-fluorophenoxy)piperidine-1-carboxylate (**37**, 99 mg, 0.24 mmol) and methyl 2-(5-fluoro-2-(3-(4,4,5,5-tetramethyl-1,3,2-dioxaborolan-2-yl)benzamido)phenyl)acetate (**29**, 100 mg, 0.24 mmol) provided the title product after column chromatography (0–5% MeOH in CH_2Cl_2) as a colorless resin in 81 mg (50%) yield. $^1\text{H NMR}$ (400 MHz, DMSO- d_6 , δ) 12.38 (s, 1H), 10.06 (s, 1H), 8.09 (s, 1H), 7.99 (d, $J = 7.7$ Hz, 1H), 7.85–7.69 (m, 1H), 7.65 (t, $J = 7.7$ Hz, 1H), 7.60 (d, $J = 10.0$ Hz, 1H), 7.45 (dd, $J = 8.8$, 5.5 Hz, 1H), 7.43–7.29 (m, 1H), 7.22 (dd, $J = 9.7$, 3.0 Hz, 1H), 7.16 (td, $J = 8.5$, 3.0 Hz, 1H), 4.78–4.44 (m, 1H), 3.96–3.70 (m, 1H), 3.69 (s, 2H), 3.53–3.32 (m, 3H), 2.01–1.70 (m, 3H), 1.57–1.43 (m, 1H), 1.15 (s, 9H). $^{13}\text{C NMR}$ (101 MHz, DMSO- d_6 , δ) 172.1, 165.2, 159.7 (d, $J = 242.0$ Hz), 153.8, 152.6 (d, $J = 252.2$ Hz), 149.3 (d, $J = 2.6$ Hz), 134.8, 134.5, 133.6 (d, $J = 8.4$ Hz), 132.8 (d, $J = 2.7$ Hz), 132.0 (d, $J = 3.2$ Hz), 128.8, 128.4 (d, $J = 8.6$ Hz), 128.1 (d, $J = 2.5$ Hz), 127.4, 127.1 (d, $J = 14.5$ Hz), 122.8, 117.9 (d, $J = 27.5$ Hz), 117.5 (d, $J = 22.8$ Hz), 116.4, 113.8 (d, $J = 22.0$ Hz), 78.3, 71.3, 45.6, 42.7, 37.2, 28.8, 27.6, 20.6. $^{19}\text{F NMR}$ (376 MHz, DMSO- d_6 , δ) –116.9, –126.3. LCMS (method a) m/z : 599.4 $[M - H]^-$, $t_R = 1.36$ min. $[\alpha]_D^{23} + 34.9$ (c 1.0, MeOH).

(*R*)-2-(2-(4'-Chloro-2'-fluoro-5'-(piperidin-3-yloxy)-[1,1'-biphenyl]-3-carboxamido)-5-fluorophenyl)acetic Acid (**19**). Following the general procedure for Boc-cleavage with HCl, (*R*)-2-(2-(3'-((1-(*tert*-butoxycarbonyl)piperidin-3-yl)oxy)-4'-chloro-2'-fluoro-[1,1'-biphenyl]-3-carboxamido)-5-fluorophenyl)acetic acid (**49**, 81 mg, 0.12 mmol) provided the title product (HCl-salt) as a colorless solid in 52 mg (81%) yield. $^1\text{H NMR}$ (400 MHz, DMSO- d_6 , δ) 12.37 (s, 1H), 10.18 (s, 1H), 9.00 (s, 1H), 8.67 (s, 1H), 8.14 (s, 1H), 8.00 (d, $J = 7.8$ Hz, 1H), 7.80 (d, $J = 7.5$ Hz, 1H), 7.70–7.62 (m, 2H), 7.59 (d, $J = 7.1$ Hz, 1H), 7.52–7.41 (m, 1H), 7.22 (dd, $J = 9.6$, 3.0 Hz, 1H), 7.16 (td, $J = 8.5$, 3.0 Hz, 1H), 4.89–4.72 (m, 1H), 3.70 (s, 2H), 3.44–3.38 (m, 1H), 3.29–3.19 (m, 1H), 3.16–2.99 (m, 2H), 2.08–1.94 (m, 2H), 1.92–1.80 (m, 1H), 1.79–1.65 (m, 1H). $^{13}\text{C NMR}$ (101 MHz, DMSO- d_6 , δ) 171.1, 165.1, 159.7 (d, $J = 240.8$ Hz), 153.4 (d, $J = 244.5$ Hz), 149.2 (d, $J = 2.8$ Hz), 134.9, 134.1, 133.6, 132.8 (d, $J = 7.8$ Hz), 132.0 (d, $J = 3.5$ Hz), 130.8 (d, $J = 31.8$ Hz), 128.8, 128.1, 127.52, 127.35 (d, $J = 14.5$ Hz), 123.3, 118.8 (d, $J = 3.5$ Hz), 118.1 (d, $J = 27.5$ Hz), 117.4 (d, $J = 22.6$ Hz), 113.8 (d, $J = 21.6$ Hz), 71.9, 45.4, 42.7, 37.4, 27.0, 18.7. $^{19}\text{F NMR}$ (376 MHz, DMSO- d_6 , δ) –117.0, –124.1. LCMS (method a) m/z : 501.2 $[M + H]^+$, $t_R = 0.97$ min. LCMS (method b) m/z : 501.2 $[M + H]^+$, $t_R = 4.53$ min. HRMS m/z : $[M + H]^+$ calcd for $\text{C}_{26}\text{H}_{24}\text{ClF}_2\text{N}_2\text{O}_4$ 501.1387; found 501.1389. $[\alpha]_D^{23} - 2.1$ (c 1.0, MeOH).

(*R*)-2-(2-(5'-((1-(*tert*-butoxycarbonyl)piperidin-3-yl)oxy)-4'-chloro-2'-difluoro-[1,1'-biphenyl]-3-carboxamido)-5-fluorophenyl)acetic Acid (**50**). According to the general procedure for Suzuki coupling, the reaction of (*R*)-*tert*-butyl 3-(5-bromo-2-chloro-4-fluorophenoxy)piperidine-1-carboxylate (**37**, 489 mg, 1.2 mmol) and methyl 2-(5-fluoro-2-(2-fluoro-3-(4,4,5,5-tetramethyl-1,3,2-dioxaborolan-2-yl)benzamido)phenyl)acetate (**30**, 600 mg, 1.2 mmol) provided the title product as a white foam in 486 mg (62%) yield. $^1\text{H NMR}$ (400 MHz, DMSO- d_6 , δ) 12.45 (s, 1H), 10.05 (s, 1H), 7.77 (t, $J = 6.4$ Hz, 1H), 7.69–7.56 (m, 2H), 7.50 (dd, $J = 8.8$, 5.6 Hz, 1H), 7.45 (t, $J = 7.7$ Hz, 1H), 7.40–7.26 (m, 1H), 7.21 (dd, $J = 9.7$, 3.0 Hz, 1H), 7.16 (td, $J = 8.5$, 2.9 Hz, 1H), 4.70–4.49 (m, 1H), 4.17–4.05 (m, 1H), 3.96–3.72 (m, 1H), 3.68 (s, 2H), 3.27–3.20 (m, 1H), 3.08–2.86 (m, 1H), 1.97–1.69 (m, 3H), 1.52–1.42 (m, 1H), 1.21 (s, 9H). $^{13}\text{C NMR}$ (101 MHz, DMSO- d_6 , δ) 171.9, 162.7, 159.3 (d, $J = 242.5$ Hz), 156.1 (d, $J = 252.5$ Hz), 153.8, 150.3 (d, $J = 234$ Hz), 149.1, 133.8, 133.1 (d, $J = 8.4$ Hz), 132.4 (d, $J = 2.6$ Hz), 130.3, 128.0 (d, $J = 8.8$ Hz), 124.8 (d, $J = 16.0$ Hz), 124.5 (d, $J = 3.9$ Hz), 122.8 (d, $J = 16.9$ Hz), 121.6 (d, $J = 17.2$ Hz), 117.7 (d, $J = 12.2$ Hz), 117.4 (d, $J = 7.8$ Hz), 117.04, 114.0, 113.8, 78.3, 71.1, 45.4, 42.7, 37.0, 28.8, 27.7, 20.5. $^{19}\text{F NMR}$ (376 MHz, DMSO- d_6 , δ) –116.84, –116.90, –123.1. LCMS (method a) m/z : 617.2 $[M - H]^-$, $t_R = 1.33$ min. $[\alpha]_D^{23} + 29.0$ (c 1.0, MeOH).

(*R*)-2-(2-(5'-((1-(*tert*-Butoxycarbonyl)piperidin-3-yl)oxy)-4'-chloro-2,2'-difluoro-[1,1'-biphenyl]-3-carboxamido)-5-fluorophenyl)acetic Acid (**20**). Following the general procedure for Boc-cleavage with HCl, (*R*)-2-(2-(5'-((1-(*tert*-Butoxycarbonyl)piperidin-3-yl)oxy)-4'-chloro-2,2'-difluoro-[1,1'-biphenyl]-3-carboxamido)-5-fluorophenyl)acetic acid (**50**, 423 mg, 0.65 mmol) provided the title product (HCl salt) as a colorless solid in 341 mg (95%) yield. ¹H NMR (400 MHz, DMSO-*d*₆, δ) 12.42 (s, 1H), 10.05 (s, 1H), 9.17 (s, 1H), 8.75 (s, 1H), 7.78 (t, *J* = 6.3 Hz, 1H), 7.72–7.62 (m, 2H), 7.54–7.41 (m, 3H), 7.21 (dd, *J* = 9.7, 3.0 Hz, 1H), 7.16 (td, *J* = 8.5, 3.1 Hz, 1H), 4.78–4.64 (m, 1H), 3.69 (s, 2H), 3.42–3.28 (m, 1H), 3.20 (dd, *J* = 12.3, 6.2 Hz, 1H), 3.14–2.99 (m, 2H), 2.05–1.90 (m, 2H), 1.89–1.79 (m, 1H), 1.77–1.67 (m, 1H). ¹³C NMR (101 MHz, DMSO-*d*₆, δ) 171.9, 162.7, 159.7 (d, *J* = 242.1 Hz), 156.0 (d, *J* = 253.3 Hz), 152.3 (d, *J* = 245.3 Hz), 148.92 (d, *J* = 2.5 Hz) 133.9, 133.1 (d, *J* = 8.4 Hz), 130.4 (d, *J* = 3.0 Hz), 128.0 (d, *J* = 8.5 Hz), 124.8 (d, *J* = 15.7 Hz), 124.5 (d, *J* = 3.7 Hz), 124.2 (d, *J* = 10.5 Hz), 122.5 (d, *J* = 16.3 Hz), 121.9 (d, *J* = 17.1 Hz), 120.0, 117.9, 117.6 (d, *J* = 6.1 Hz), 117.4, 113.9 (d, *J* = 22.3 Hz), 71.9, 45.2, 42.7, 37.0, 26.9, 18.6. ¹⁹F NMR (376 MHz, DMSO-*d*₆, δ) –116.6, –116.8, –120.8. LCMS (method a) *m/z*: 519.1 [M + H]⁺, *t*_R = 0.81 min. LCMS (method b) *m/z*: 519.1 [M + H]⁺, *t*_R = 3.66 min. HRMS *m/z*: [M + H]⁺ calcd for C₂₆H₂₃ClF₃N₂O₄ 519.1293; found 519.1293. [α]_D²³ –1.3 (c 1.0, MeOH).

BIOLOGY

SUCNR1 GTPγS Assay. Assays were done as described (Haffke et al. 2019)²⁰ using membranes from stably transfected Chem1 or CHO-K1 cells expressing human or rat SUCNR1, respectively. The final assay mixture in 96-well Optiplates (Perkin Elmer) contained 15 μg of rat or human SUCNR1 membranes, wheat germ-agglutinin-coated scintillation proximity assay beads (Perkin Elmer), 200 pM [³⁵S]GTPγS (Perkin Elmer), 20 mM HEPES pH 7.4, 100 mM NaCl, 10 mM MgCl₂, 25 μg/mL saponin, 10 μM GDP, 0.1% fat-free bovine serum albumin, 50 μM succinate, and the test compound. After incubation for 60 min at room temperature sealed plates were centrifuged for 10 min at 1200 rpm and the radioactivity was counted (TopCount NXT; Perkin Elmer). IC₅₀ values were determined from eight-point concentration–response curves using GraphPad Prism.

In Vivo Experiments. All animals used were 5–12 weeks of age and were maintained in the specific pathogen-free facilities. All animal studies were performed in accordance with the animal experimentation guidelines and laws laid down by the Swiss Federal and Cantonal Authorities.

In Vivo Pharmacokinetic Studies in Mice. Pharmacokinetic studies were conducted using male C57/BL6 mice. For 1 mg/kg intravenous dosing, compounds were formulated as a solution (NMP:plasma (10:90)) and mice (*n* = 3 per group) were administered compounds by bolus injection; the dose volume was 5 mL/kg. For oral dosing, compounds were formulated as a suspension (MC:water:Tween80 (0.5:99:0.5)). Mice (*n* = 3 per group) were administered by oral gavage; the dose volume was 10 mL/kg. Serial intravenous blood samples were taken at 0.083, 0.25, 0.5, 1, 2, 4, 7, and 24 h. For the oral arm blood samples were taken at 0.25, 0.5, 1, 2, 4, 7, and 24 h; precipitated with acetonitrile; and stored at –20 °C prior to liquid chromatography–mass spectrometry (LC–MS)/MS analysis. Pharmacokinetic parameters were calculated by noncompartmental analysis. Pharmacokinetic studies with compounds **8** and **9** were described previously.²⁸

Protein Expression, Purification, and Crystallization of Humanized Rat SUCNR1 in Complex with **20.** The expression, purification, and crystallization of the humanized

rat SUCNR1–Nanobody6 complex were performed as described previously with the following modifications for complex formation and crystallization:²⁰

Compound **5** was added to purified humanized rat SUCNR1 to a final concentration of 1 mM from a 100 mM stock solution in DMSO, giving a final DMSO concentration of 1% (v/v). The receptor was mixed with a 1.2 M excess of purified Nanobody6, incubated on ice for 30 min. The complex was further purified without any antagonist by size-exclusion chromatography on a Superose6 Increase 10/300 GL column (GE Healthcare) equilibrated in 25 mM HEPES pH 7.5, 800 mM NaCl, 10% (w/v) glycerol, 0.002% (w/v) LMNG, and 0.0004% (w/v) CHS. Peak fractions were pooled and concentrated using a 100 kDa MWCO concentrator (Millipore) to a final concentration of 30 mg/mL. The complex was flash-frozen in liquid nitrogen in small aliquots and stored at –80 °C until crystallization.

The rat SUCNR1–Nanobody6 complex was reconstituted in the lipidic cubic phase (LCP) by mixing protein at 30 mg/mL with monoolein:cholesterol (9:1) (w:w) at a 2:3 ratio (v:w) in 50 μL Hamilton syringes using the two-syringe method. Crystallization trials were performed using Innovadyne SD-2 vapor diffusion plates and dispensed using an Oryx8 crystallization robot (Douglas Instruments). Protein-laden LCP (50 nL) was covered with 2.25 μL of precipitant, containing 200 μM **20**, and incubated at 20 °C in an RI-1000 imager (Formulatrix). First crystals appeared within 24 h and grew to a maximum size of 40 μm × 40 μm × 40 μm in 10 days in 50 mM 2-[(2-amino-2-oxoethyl)-(carboxymethyl)-amino]acetic acid (ADA) pH 7.0, 28% (w/v) poly(ethylene glycol) monomethyl ether (PEG MME) 550, 0.55 M (NH₄)₂SO₄, 200 μM **20**, and 2% (v/v) DMSO. Crystals were directly collected from the LCP bolus with MiTeGen micromount loops and flash-frozen in liquid nitrogen.

Data Collection, Structure Solution and Refinement. Data for the humanized rat SUCNR1–Nanobody6–**20** complex were collected at PXII at the Swiss Light Source, Villigen, Switzerland, using a 10 μm diameter beam at a wavelength of 0.999 Å on a Dectris Eiger-16M detector. Crystals were exposed for 0.05 s per 0.1° oscillation per frame using an attenuated beam to reduce radiation damage. Datasets were integrated, scaled, and merged using XDS and XSCALE in autoPROC and aP_Scale (Global Phasing). Data collection and refinement statistics are reported in Extended Data Table S1 (Supporting Information). The structure was solved by molecular replacement in Phaser using the structure of the humanized rat SUCNR1–Nanobody6–NF-56-EJ40 (**7**) complex (PDB 6RNK) as a search model. The structural model was adjusted by repetitive rounds of manual model building in Coot and refinement against the anisotropic-scaled data in Buster (Global Phasing). Structure factors and coordinates of the humanized rat GRP91–Nanobody6–**20** complex were deposited in the Protein Data Bank (PDB) under accession codes 6Z10.

Following high-throughput assays were performed according to the described procedures: PAMPA,²² LogD_{7.4},²³ and UV-metric pK_a.³⁶

Plasma Protein Binding (PPB). Compounds, dissolved in DMSO, were added to the plasma to achieve a concentration of 5 μM and 0.5% DMSO. Plasma samples were placed in one chamber of the rapid equilibrium dialysis (RED) device. Phosphate-buffered saline (100 mM) containing 0.5% DMSO was placed in the other chamber. The RED device was shaken

at 250 rpm at 37 °C with 5% CO₂ for 4 h to reach equilibrium. After the incubation, 0.45 μL of the sample was removed from each side of the membrane. An equal volume of 100 mM phosphate buffer containing 0.5% DMSO was added to the plasma sample. An equal volume of plasma containing 0.5% DMSO was also added to the buffer sample. Samples were protein-precipitated with 180 μL of chilled methanol (containing the internal standard 0.55 μM metoprolol). After being shaken, the samples were centrifuged at 2000g for 30 min, and 20 μL of the supernatant was removed and diluted with 20 μL of water prior to LC–MS/MS analysis. The fraction unbound in plasma (fu) was calculated by dividing the concentration in the buffer chamber by the concentration in the plasma chamber.

Docking Studies. Docking studies were carried out using Glide SP at standard settings (cite: Schrödinger Release 2019-2: Glide, Schrödinger, LLC, New York, NY, 2019). Figures were prepared using PyMOL (cite: The PyMOL Molecular Graphics System, Version 2.0 Schrödinger, LLC).

■ ASSOCIATED CONTENT

SI Supporting Information

The Supporting Information is available free of charge at <https://pubs.acs.org/doi/10.1021/acs.jmedchem.0c01020>.

HPLC and NMR charts and X-ray crystallographic data for compounds **9**, **10**, and **20** as well as SUCNR1-bound **20** (PDF)

Molecular formula strings (CSV)

Accession Codes

Atomic coordinates and structure factors for the crystal structures of compounds **9**, **10**, and **20** can be accessed using the following codes: CCDC 2009710 (**9**), CCDC 2009711 (**10**), and CCDC 2009712 (**20**). For compound **20** bound to humanized rat SUCNR1, the PDB code is 6Z10. The authors will release the atomic coordinates upon article publication.

■ AUTHOR INFORMATION

Corresponding Author

Juraj Velcicky – Novartis Institutes for BioMedical Research, CH-4002 Basel, Switzerland; orcid.org/0000-0001-6564-1448; Email: juraj.velcicky@novartis.com

Authors

Rainer Wilcken – Novartis Institutes for BioMedical Research, CH-4002 Basel, Switzerland; orcid.org/0000-0002-6159-1460

Simona Cotesta – Novartis Institutes for BioMedical Research, CH-4002 Basel, Switzerland

Philipp Janser – Novartis Institutes for BioMedical Research, CH-4002 Basel, Switzerland

Achim Schlapbach – Novartis Institutes for BioMedical Research, CH-4002 Basel, Switzerland

Trixie Wagner – Novartis Institutes for BioMedical Research, CH-4002 Basel, Switzerland

Philippe Piechon – Novartis Institutes for BioMedical Research, CH-4002 Basel, Switzerland

Frederic Villard – Novartis Institutes for BioMedical Research, CH-4002 Basel, Switzerland

Rochdi Bouhelal – Novartis Institutes for BioMedical Research, CH-4002 Basel, Switzerland

Fabian Piller – Novartis Institutes for BioMedical Research, CH-4002 Basel, Switzerland

Stephanie Harlfinger – Novartis Institutes for BioMedical Research, CH-4002 Basel, Switzerland

Rowan Stringer – Novartis Institutes for BioMedical Research, CH-4002 Basel, Switzerland

Dominique Fehlmann – Novartis Institutes for BioMedical Research, CH-4002 Basel, Switzerland

Klemens Kaupmann – Novartis Institutes for BioMedical Research, CH-4002 Basel, Switzerland

Amanda Littlewood-Evans – Novartis Institutes for BioMedical Research, CH-4002 Basel, Switzerland

Matthias Haffke – Novartis Institutes for BioMedical Research, CH-4002 Basel, Switzerland

Nina Gommermann – Novartis Institutes for BioMedical Research, CH-4002 Basel, Switzerland

Complete contact information is available at:

<https://pubs.acs.org/10.1021/acs.jmedchem.0c01020>

Author Contributions

The manuscript was written through contributions of all authors. All authors have given approval to the final version of the manuscript.

Funding

The authors declare no competing financial interest, and all work described was funded by Novartis Institutes for BioMedical Research Inc.

Notes

The authors declare no competing financial interest.

■ ACKNOWLEDGMENTS

We thank Daniel Pflieger, Günter Schwalm, Bernard Faller, Gaelle Chenal, and Harald Schroeder for their assistance during the preparation of this manuscript. We would also like to thank Stephane Rodde and Damien Hubert for the physicochemical measurements and Corinne Marx for HRMS measurements.

■ ABBREVIATIONS USED

CHO-K1, Chinese hamster ovary cells; CHS, cholesteryl hemisuccinate; DIAD, diisopropyl azodicarboxylate; DIPEA, *N,N*-diisopropylethylamine; dn, dose-normalized; dppf, 1,1'-ferrocenediyl-bis(diphenylphosphine); HEPES, 4-(2-hydroxyethyl)-1-piperazineethanesulfonic acid; HIF1 α , hypoxia-inducible factor 1 α ; extrap, extrapolated; LMNG, lauryl maltose neopentyl glycol; MC, methyl cellulose; MWCO, molecular weight cut-off; Pin, pinacol

■ REFERENCES

(1) He, W.; Miao, F. J.-P.; Lin, D. C.-H.; Schwandner, R. T.; Wang, Z.; Gao, J.; Chen, J.-L.; Tian, H.; Ling, L. Citric acid cycle intermediates as ligands for orphan G-protein-coupled receptors. *Nature* **2004**, *429*, 188–193.

(2) de Castro Fonseca, M.; Aguiar, C. J.; da Rocha Franco, J. A.; Gingold, R. N.; Leite, M. F. GPR91: expanding the frontiers of Krebs cycle intermediates. *Cell Commun. Signaling* **2016**, *14*, No. 3.

(3) Haas, R.; Cucchi, D.; Smith, J.; Pucino, V.; Macdougall, C. E.; Mauro, C. Intermediates of metabolism: from bystanders to signalling molecules. *Trends Biochem. Sci.* **2016**, *41*, 460–471.

(4) Tannahill, G. M.; Curtis, A. M.; Adamik, J.; Palsson-McDermott, E. M.; McGettrick, A. F.; Goel, G.; Frezza, C.; Bernard, N. J.; Kelly, B.; Foley, N. H.; Zheng, L.; Gardet, A.; Tong, Z.; Jany, S. S.; Corr, S. C.; Haneklaus, M.; Caffrey, B. E.; Pierce, K.; Walmsley, S.; Beasley, F.

- C.; Cummins, E.; Nizet, V.; Whyte, M.; Taylor, C. T.; Lin, H.; Masters, S. L.; Gottlieb, E.; Kelly, V. P.; Clish, C.; Auron, P. E.; Xavier, R. J.; O'Neill, L. A. J. Succinate is an inflammatory signal that induces IL-1 β through HIF-1 α . *Nature* **2013**, *496*, 238–242.
- (5) Ariza, A. C.; Deen, P. M. T.; Robben, J. H. The succinate receptor as a novel therapeutic target for oxidative and metabolic stress-related conditions. *Front. Endocrinol.* **2012**, *3*, 1–8.
- (6) Cho, E.-H. Succinate as a regulator of hepatic stellate cells in liver fibrosis. *Front. Endocrinol.* **2018**, *9*, 455.
- (7) Macaulay, I. C.; Tijssen, M. R.; Thijssen-Timmer, D. C.; Gusnanto, A.; Steward, M.; Burns, P.; Langford, C. F.; Ellis, P. D.; Dudbridge, F.; Zwaginga, J. J.; Watkins, N. A.; van der Schoot, C. E.; Ouwehand, W. H. Comparative gene expression profiling of in vitro differentiated megakaryocytes and erythroblasts identifies novel activatory and inhibitory platelet membrane proteins. *Blood* **2007**, *109*, 3260–3269.
- (8) Toma, I.; Kang, J. J.; Sipos, A.; Vargas, S.; Bansal, E.; Hanner, F.; Meer, E.; Peti-Peterdi, J. Succinate receptor GPR91 provides a direct link between high glucose levels and renin release in murine and rabbit kidney. *J. Clin. Invest.* **2008**, *118*, 2526–2534.
- (9) Vargas, S. L.; Toma, I.; Kang, J. J.; Meer, E. J.; Peti-Peterdi, J. Activation of the succinate receptor GPR91 in macula densa cells causes renin release. *J. Am. Soc. Nephrol.* **2009**, *20*, 1002–1011.
- (10) McCreath, K. J.; Espada, S.; Gálvez, B. G.; Benito, M.; de Molina, A.; Sepúlveda, P.; Cervera, A. M. Targeted disruption of the SUCNR1 metabolic receptor leads to dichotomous effects on obesity. *Diabetes* **2015**, *64*, 1154–1167.
- (11) Sapiha, P.; Sirinyan, M.; Hamel, D.; Zaniolo, K.; Joyal, J. S.; Cho, J.-H.; Honoré, J. C.; Kermorvant-Duchemin, E.; Varma, D. R.; Tremblay, S.; Leduc, M.; Rihakova, L.; Hardy, P.; Klein, W. H.; Mu, X.; Mamer, O.; Lachapelle, P.; Di Polo, A.; Beauséjour, C.; Andelfinger, G.; Mitchell, G.; Sennlaub, F.; Chemtob, S. The succinate receptor GPR91 in neurons has a major role in retinal angiogenesis. *Nat. Med.* **2008**, *14*, 1067–1076.
- (12) Rubic, T.; Lametschwandner, G.; Jost, S.; Hinteregger, S.; Kund, J.; Carballido-Perrig, N.; Schwärzler, C.; Junt, T.; Voshol, H.; Meingassner, J. G.; Mao, X.; Werner, G.; Rot, A.; Carballido, J. M. Triggering the succinate receptor GPR91 on dendritic cells enhances immunity. *Nat. Immunol.* **2008**, *9*, 1261–1269.
- (13) Saraiva, A. L.; Veras, F. P.; Peres, R. S.; Talbot, J.; de Lima, K. A.; Luiz, J. P.; Carballido, J. M.; Cunha, T. M.; Cunha, F. Q.; Ryffel, B.; Alves-Filho, J. C. Succinate receptor deficiency attenuates arthritis by reducing dendritic cell traffic and expansion of Th17 cells in the lymph nodes. *FASEB J.* **2018**, *32*, 6550–6558.
- (14) Kim, S.; Hwang, J.; Xuan, J.; Jung, Y. H.; Cha, H.-S.; Kim, K. H. Global metabolite profiling of synovial fluid for the specific diagnosis of rheumatoid arthritis from other inflammatory arthritis. *PLoS One* **2014**, *9*, No. e97501.
- (15) Littlewood-Evans, A.; Sarret, S.; Apfel, V.; Loesle, P.; Dawson, J.; Zhang, J.; Muller, A.; Tigani, B.; Kneuer, R.; Patel, S.; Valeaux, S.; Gommermann, N.; Rubic-Schneider, T.; Junt, T.; Carballido, J. M. GPR91 senses extracellular succinate released from inflammatory macrophages and exacerbates rheumatoid arthritis. *J. Exp. Med.* **2016**, *213*, 1655–1662.
- (16) Bhuniya, D.; Umrani, D.; Dave, B.; Salunke, D.; Kukreja, G.; Gundu, J.; Naykodi, M.; Shaikh, N. S.; Shitole, P.; Kurhade, S.; De, S.; Majumdar, S.; Reddy, S. B.; Tambe, S.; Shejul, Y.; Chugh, A.; Palle, V. P.; Mookhtiar, K. A.; Cully, D.; Vacca, J.; Chakravarty, P. K.; Nargund, R. P.; Wright, S. D.; Graziano, M. P.; Singh, S. B.; Roy, S.; Cai, T.-Q. Discovery of a potent and selective small molecule hGPR91 antagonist. *Bioorg. Med. Chem. Lett.* **2011**, *21*, 3596–3602.
- (17) Trauelsen, M.; Ulven, E. R.; Hjorth, S. A.; Brvar, M.; Monaco, C.; Frimurer, T. M.; Schwartz, T. W. Receptor structure-based discovery of non-metabolite agonists for the succinate receptor GPR91. *Mol. Metab.* **2017**, *6*, 1585–1596.
- (18) Ulven, E. R.; Trauelsen, M.; Brvar, M.; Lückmann, M.; Bielefeldt, L. Ø.; Jensen, L. K. I.; Schwartz, T. W.; Frimurer, T. M. Structure-activity investigations and optimisations of nonmetabolite agonists for the Succinate Receptor 1. *Sci. Rep.* **2018**, No. 10010.
- (19) Geubelle, P.; Gilissen, J.; Dilly, S.; Poma, L.; Dupuis, N.; Laschet, C.; Abboud, D.; Inoue, A.; Jouret, F.; Pirotte, B.; Hanson, J. Identification and pharmacological characterization of succinate receptor agonists. *Br. J. Pharmacol.* **2017**, *174*, 796–808.
- (20) Haffke, M.; Fehlmann, D.; Rummel, G.; Boivineau, J.; Duckely, M.; Gommermann, N.; Cotesta, S.; Sirockin, F.; Freuler, F.; Littlewood-Evans, A.; Kaupmann, K.; Jaakola, V.-P. Structural basis of species-selective antagonist binding to the succinate receptor. *Nature* **2019**, *574*, 581–585.
- (21) *Drug-like Properties: Concepts, Structure Design and Methods from ADME to Toxicity Optimization*, 2nd ed.; Di, L.; Kerns, E., Eds.; Academic press: London, 2016.
- (22) Wohnsland, F.; Faller, B. High-throughput permeability pH profile and high-throughput alkane/water log P with artificial membranes. *J. Med. Chem.* **2001**, *44*, 923–930.
- (23) Low, Y. W. I.; Blasco, F.; Vachaspati, P. Optimised method to estimate octanol water distribution coefficient (logD) in a high throughput format. *Eur. J. Pharm. Sci.* **2016**, *92*, 110–116.
- (24) Gillis, E. P.; Eastman, K. J.; Hill, M. D.; Donnelly, D. J.; Meanwell, N. A. Applications of fluorine in medicinal chemistry. *J. Med. Chem.* **2015**, *58*, 8315–8359.
- (25) Velcicky, J.; Schlapbach, A.; Heng, R.; Revesz, L.; Pflieger, D.; Blum, E.; Hawtin, S.; Huppertz, C.; Feifel, R.; Hersperger, R. Modulating ADME properties by fluorination: MK2 inhibitors with improved oral exposure. *ACS Med. Chem. Lett.* **2018**, *9*, 392–396.
- (26) Müller, K. Simple vector considerations to assess the polarity of partially fluorinated alkyl and alkoxy groups. *Chimia* **2014**, *68*, 356–362.
- (27) Ziegler, B. E.; Lecours, M.; Marta, R. A.; Featherstone, J.; Fillion, E.; Hopkins, W. S.; Steinmetz, V.; Keddie, N. S.; O'Hagan, D.; McMahon, T. B. Janus face aspect of all-cis 1,2,3,4,5,6-hexafluorocyclohexane dictates remarkable anion and cation interactions in the gas phase. *J. Am. Chem. Soc.* **2016**, *138*, 7460–7463.
- (28) Karki, R. G.; Powers, J.; Mainolfi, N.; Anderson, K.; Belanger, D. B.; Liu, D.; Ji, N.; Jendza, K.; Gelin, C. F.; Mac Sweeney, A.; Solovay, C.; Delgado, O.; Crowley, M.; Liao, S. M.; Argikar, U. A.; Flohr, S.; La Bonte, L. R.; Lorthiois, E. L.; Vulpetti, A.; Brown, A.; Long, D.; Prentiss, M.; Gradoux, N.; de Erkenez, A.; Cumin, F.; Adams, C.; Jaffee, B.; Mogi, M. Design, synthesis, and preclinical characterization of selective Factor D inhibitors targeting the alternative complement pathway. *J. Med. Chem.* **2019**, *62*, 4656–4668.
- (29) Lorthiois, E.; Roache, J.; Barnes-Seeman, D.; Altmann, E.; Hassiepen, U.; Turner, G.; Duvadie, R.; Hornak, V.; Karki, R. G.; Schiering, N.; Weihofen, W. A.; Perruccio, F.; Calhoun, A.; Fazal, T.; Dedic, D.; Durand, C.; Dussauge, S.; Fettes, K.; Tritsch, F.; Dentel, C.; Druet, A.; Liu, D.; Kirman, L.; Lachal, J.; Namoto, K.; Bevan, D.; Mo, R.; Monnet, G.; Muller, L.; Zessis, R.; Huang, X.; Lindsley, L.; Currie, T.; Chiu, Y.-H.; Fridrich, C.; Delgado, P.; Wang, S.; Hollis-Symynkywicz, M.; Berghausen, J.; Williams, E.; Liu, H.; Liang, G.; Kim, H.; Hoffmann, P.; Hein, A.; Ramage, P.; D'Arcy, A.; Harlfinger, S.; Renatus, M.; Ruedisser, S.; Feldman, D.; Elliott, J.; Sedrani, R.; Maibaum, J.; Adams, C. M. Structure-based design and pre-clinical characterization of selective and orally bioavailable Factor XIa inhibitors: Demonstrating the power of an integrated S1 protease family approach in drug discovery. *J. Med. Chem.* **2020**, *63*, 8088–8113.
- (30) Vulpetti, A.; Ostermann, N.; Randl, S.; Yoon, T.; Mac Sweeney, A.; Cumin, F.; Lorthiois, E.; Rüdissler, S.; Erbel, P.; Maibaum, J. Discovery and design of first benzylamine-based ligands binding to an unlocked conformation of the Complement Factor D. *ACS Med. Chem. Lett.* **2018**, *9*, 490–495.
- (31) Edmonson, S. D.; Mastracchio, A.; Beconi, M.; Colwell, L. F., Jr.; Habulihaz, B.; He, H.; Kumar, S.; Leiting, B.; Lyons, K. A.; Mao, A.; Marsilio, F.; Patel, R. A.; Wu, J. K.; Zhu, L.; Thornberry, N. A.; Weber, A. E.; Parmee, E. R. Potent and selective proline derived dipeptidyl peptidase IV inhibitors. *Bioorg. Med. Chem. Lett.* **2004**, *14*, 5151–5155.
- (32) Xu, J.; Wei, L.; Mathvink, R.; He, J.; Park, Y. J.; He, H.; Leiting, B.; Lyons, K. A.; Marsilio, F.; Patel, R. A.; Wu, J. K.; Thornberry, N.

A.; Weber, A. E. Discovery of potent and selective phenylalanine based dipeptidyl peptidase IV inhibitors. *Bioorg. Med. Chem. Lett.* **2005**, *15*, 2533–2536.

(33) Caudana, F.; Ermondi, G.; Vallaro, M.; Shalaeva, M.; Caron, G. Permeability prediction for zwitterions via chromatographic indexes and classification into ‘certain’ and ‘uncertain’. *Future Med. Chem.* **2019**, *11*, 1553–1563.

(34) Bohnert, T.; Gan, L.-S. Plasma protein binding: from discovery to development. *J. Pharm. Sci.* **2013**, *102*, 2953–2994.

(35) Yang, Z.; Li, Q.; Yang, G. Zwitterionic structures: from physicochemical properties toward computer-aided drug designs. *Future Med. Chem.* **2016**, *8*, 2245–2262.

(36) Gedeck, P.; Lu, Y.; Skolnik, S.; Rodde, S.; Dollinger, G.; Jia, W.; Berellini, G.; Vianello, R.; Faller, B.; Lombardo, F. Benefit of retraining pKa models studied using internally measured data. *J. Chem. Inf. Model.* **2015**, *55*, 1449–1459.

(37) Tam, K. Y.; Avdeef, A.; Tsinman, O.; Sun, N. The permeation of amphoteric drugs through artificial membranes - An in combo absorption model based on paracellular and transmembrane permeability. *J. Med. Chem.* **2010**, *53*, 392–401.

(38) Nielsen, D. S.; Shepherd, N. E.; Xu, W.; Lucke, A. J.; Stoermer, M. J.; Fairlie, D. P. Orally absorbed cyclic peptides. *Chem. Rev.* **2017**, *117*, 8094–8128.

(39) Kumar, S.; Nussinov, R. Close-range electrostatic interactions in proteins. *ChemBioChem* **2002**, *3*, 604–617.

(40) Caron, G.; Kihlberg, J.; Ermondi, G. Intramolecular hydrogen bonding: An opportunity for improved design in medicinal chemistry. *Med. Res. Rev.* **2019**, *39*, 1707–1729.

(41) Brameld, K. A.; Kuhn, B.; Reuter, D. C.; Stahl, M. Small molecule conformational preferences derived from crystal structure data. A medicinal chemistry focused analysis. *J. Chem. Inf. Model.* **2008**, *48*, 1–24.

(42) Vashchenko, A.; Smirnov, V.; Semenova, N.; Schmidt, E. Unusual structure of a biphenyl fragment: the important role of weak interactions. *Acta Crystallogr., Sect. C: Struct. Chem.* **2019**, *75*, 1454–1458.

(43) Alex, A.; Millan, D. S.; Perez, M.; Wakenhut, F.; Whitlock, G. A. Intramolecular hydrogen bonding to improve membrane permeability and absorption in beyond rule of five chemical space. *Med. Chem. Commun.* **2011**, *2*, 669–674.

(44) Udvarhelyi, A.; Rodde, S.; Wilcken, R. ReSCoSS: A flexible quantum chemistry workflow identifying relevant solution conformers of drug-like molecules. *J. Comput.-Aided Mol. Des.* **2020**, DOI: 10.1007/s10822-020-00337-7.

(45) Danelius, E.; Poongavanam, V.; Peintner, S.; Wieske, L. H. E.; Erdélyi, M.; Kihlberg, J. Solution conformations explain the chameleonic behaviour of macrocyclic drugs. *Chem.–Eur. J.* **2020**, *26*, 5231–5244.

(46) Sebastiano, M. R.; Doak, B. C.; Backlund, M.; Poongavanam, V.; Over, B.; Ermondi, G.; Caron, G.; Matsson, P.; Kihlberg, J. Impact of dynamically exposed polarity on permeability and solubility of chameleonic drugs beyond the Rule of 5. *J. Med. Chem.* **2018**, *61*, 4189–4202.

(47) Kenda, B.; Quesnel, Y.; Ates, A.; Michel, P.; Turet, L.; Mercier, J. 2-Oxo-1-pyrrolidine derivatives. WO2006/128692 A2, 2006.

(48) Swamy, K. C. K.; Kumar, N. N. B.; Balaraman, E.; Kumar, K. V. P. Mitsunobu and related reactions: advances and applications. *Chem. Rev.* **2009**, *109*, 2551–2651.